Original Article

MYC, BCL2 and BCL6 co-localisation patterns at single-cell resolution underlie their prognostic significance in diffuse large B-cell lymphoma

Authors: Michal Marek Hoppe[1], Fan Shuangyi[2], Patrick Jaynes[1], Yanfen Peng[1], Phuong Mai Hoang[1], Liu Xin[3], Sanjay De Mel[3,4], Limei Poon[3,4], Esther Chan[3,4], Joanne Lee[3,4], Yen Lin Chee[3,4], Ong Choon Kiat[5], Tiffany Tang[6], Lim Soon Thye[6], Nicholas Francis Grigoropoulos[7], Soo-Yong Tan[2,4], Susan Swee-Shan Hue[2], Sheng-Tsung Chang[8], Shih-Sung Chuang[8], Shaoying Li[9], Joseph D. Khoury[9], Hyungwon Choi[10], Pedro Farinha[11], Anja Mottok[12], David W. Scott[11], Wee-Joo Chng[1,4,10], Claudio Tripodo[13], Siok-Bian Ng[1,2,4], Anand D. Jeyasekharan[1,3,4*]

Affiliations:

[1] Cancer Science Institute of Singapore, National University of Singapore, Singapore
[2] Department of Pathology, Yong Loo Lin School of Medicine, National University of Singapore, Singapore
[3] Department of Haematology-Oncology, National University Health System, Singapore
[4] National University Cancer Institute, Singapore, National University Health System, Singapore
[5]Division of Cellular and Molecular Research, National Cancer Centre Singapore, Singapore
[6]Division of Medical Oncology, National Cancer Centre Singapore, Singapore
[7]Department of Haematology, Singapore General Hospital, Singapore
[8]Department of Pathology, Chi-Mei Medical Center, Tainan City, Taiwan
[9]Department of Hematopathology, Division of Pathology and Laboratory Medicine, The University of Texas MD Anderson Cancer Center, Houston, Texas, USA
[10]Department of Medicine, Yong Loo Lin School of Medicine, National University of Singapore, Singapore
[11]BC Cancer Research Centre, Vancouver, Canada
[12] Institute of Human Genetics, University Medical Center and University of Ulm, Ulm, Germany
[13]University of Palermo, Tumor Immunology Unit, Palermo, Italy
* To whom correspondence is to be addressed

Corresponding Author: Dr Anand D. Jeyasekharan; Cancer Science Institute of Singapore, Centre for Translational Medicine (MD6) #13-01G, 14 Medical Drive, Singapore 117599; ; csiadj@nus.edu.sg; T: +65 6516 5094

Running title: MYC/BCL2/BCL6 localisation in DLBCL at single cell resolution

Keywords: Spectral Imaging, single-cell analysis, digital pathology, quantitative immunofluorescence, MYC, DLBCL

Financial Support: ADJ was supported by the Singapore Ministry of Health's National Medical Research Council Transition Award (NMRC/TA/0052/2016). Work in ADJ's laboratory is funded by a core grant from the Cancer Science Institute of Singapore, National University of Singapore through the National Research Foundation Singapore and the Singapore Ministry of Education under its Research Centres of Excellence initiative, as well as by Singapore Ministry of Health's National Medical Research Council 'Singapore lYMPHoma translatiONal studY (SYMPHONY)' Open Fund Large Collaborative Grant (MOH-000205-03).

Conflicts of Interest: ADJ has received consultancy fees from Turbine Ltd, AstraZeneca, Janssen and MSD, along with travel funding from Perkin Elmer, and research funding from Janssen. The other co-authors have no relevant conflicts of interest to declare.

This manuscript includes:

Main Text: 5678 words

Tables 1 to 1

Figures 1 to 7

Supplementary tables 1 to 6

Supplementary figures 1 to 5

Abstract

MYC, BCL2 and BCL6 expression are prognostic indicators in diffuse large B-cell lymphomas (DLBCL). However, it remains unknown whether MYC, BCL2 and BCL6 are co-expressed at the single-cell level in DLBCL, and if patterns of co-expression determine prognosis. We used fluorescence-based quantitative immunohistochemistry (qIHC) to demonstrate that MYC(M), BCL2(2) and BCL6(6) show disordered patterns of co-expression at single-cell resolution in DLBCL, distinct from those of non-malignant lymphoid tissues. Among possible permutations of co-localisation, the sub-population M+2+6- was independently predictive of poor survival in multiple cohorts of DLBCL. Interestingly, these sub-populations could be mathematically predicted from single marker data, with high correlation to observed co-localisation by multiplex IHC. Via this mathematical model, the association of M+2+6- extent with poor survival was independently validated using both gene expression datasets and conventional IHC scores. These results clarify the interrelationship of MYC, BCL2 and BCL6 in determining outcome of DLBCL, with biological and diagnostic implications.

[150/150]

Statement of significance

This first analysis of MYC, BCL2 and BCL6 spatial single-cell co-localisation in DLBCL addresses a long-standing debate about thresholds of prognostic significance for these markers, offering a quantitative solution for patient stratification. The novel modelling approach for estimating cellular co-expression from single marker data may be widely applicable in cancer research.

[50/50]

Introduction

Diffuse large B-cell lymphoma (DLBCL) is the most common aggressive lymphoma worldwide (1). First-line chemoimmunotherapy with R-CHOP (rituximab with cyclophosphamide, doxorubicin, vincristine and prednisone) leads to clearance of disease in the majority of patients (1). However, a significant proportion of cases (up to 40%) are either refractory to or relapse after first-line R-CHOP treatment (2). Therapeutic options improving on R-CHOP for DLBCL therefore represent an unmet clinical need. However, numerous randomized phase III trials to improve on R-CHOP therapy have been unsuccessful, partly due to the lack of predictive biomarkers to enrich a trial for poor-prognosis cases (3-8). There is a clear requirement to refine markers of poor prognosis in DLBCL.

Expression of the oncogenes MYC, BCL2 and BLC6 have long been recognized to be prognostic in DLBCL (9-11). In particular, DLBCL with expression of MYC and BCL2, termed Double Expressor Lymphomas (DEL) (12) have a poor prognosis on standard R-CHOP therapy (9,12-15), and occur in 20-30% of patients (16). The expression of BCL6 appears to have protective effect in DEL cases (11,17). However, the utility of this DEL phenotype in clinical trial patient selection is marred by controversies in the definition of what constitutes “positivity” for MYC and BCL2; the qualitative and subjective nature of visual chromogenic immunohistochemistry (IHC) resulted in wide variability of this effect among studies. Despite advances in digital pathology, there are to-date no large studies validating automated IHC algorithms to address the quantitation of MYC/BCL2 and BCL6.

Another important unanswered question about these oncogenes is to what extent the expression of MYC, BCL2 and BCL6 actually occurs in the same or distinct tumour cells within a single case. Clonal heterogeneity is a common feature of cancer and it is not known for instance if DELs actually represent two independent clonal phenotypes within a lymphoma. Analysing spatial co-expression using conventional IHC and visual scores is challenging because of the limitations intrinsic to discerning and scoring relative amounts of 2 or 3 colours within in a single area of interest (e.g. the nucleus of a cell). As a result, the staining of MYC, BCL2 and BCL6 is reported independently and with respect to the overall tumour cellularity. How these markers prognostically interact at the single-cell level in the context of DLBCL remains unexplored.

Multiplexed imaging and automated analysis provides a possible solution to address both the issues of quantitation and co-localisation for these relevant markers. Multispectral imaging has since been used widely in cancer research to quantitate protein expression in-situ and to identify

distinct immune infiltrating cells within tumours(18-20). This technique has primarily been used in epithelial cancer research, but is particularly useful for lymphomas given the intrinsic difficulty in distinguishing between tumour cells and immune infiltrates in these cancers as compared to solid cancers.

In this study, we use quantitative immunohistochemistry (qIHC) through multispectral fluorescence imaging to simultaneously assess MYC, BCL2 and BCL6 expression with single-cell resolution in control non-malignant tonsils and in multiple DLBCL cohorts. We observed distinct co-expression patterns of these oncogenes between tonsil and DLBCL tissues. The single-cell resolution of each stain allowed us to identify sub-populations based on the possible permutations of MYC, BCL2 and BCL6 co-localisation, with distinct prognostic outcomes. Furthermore, we discovered that the co-localisation pattern of the three markers in DLBCL could be best explained by the expression of each marker being independently regulated of each other. As a direct result of this, the percentage of co-expressing cells within each tumour could be mathematically predicted. Using mathematical modelling to predict the percentage of co-expressing cells in RNA datasets as well as an IHC dataset with single-marker staining information, we were able to validate the influence of a specific sub-population of MYC+BCL2+BCL6- cells on prognosis in a variety of heterogenous data-sets.

Results

Distinct patterns of MYC, BCL2 and BCL6 co-expression in reactive lymphoid tissue compared to DLBCL

To simultaneously assess MYC, BCL2 and BCL6 expression, we performed quantitative immunohistochemistry (qIHC) using a sequential OPAL-TSA staining protocol (see methods for details) and multispectral microscopy on the Vectra platform. We probed for MYC, BCL2 and BCL6 protein expression as well as the B-cell specific marker CD20 and the proliferation marker Ki67. In order to accurately interpret the staining pattern of these markers in DLBCL, we first investigated how they are distributed and associated in benign lymphoid tissue, using tonsil samples with reactive follicular hyperplasia. The spectral unmixing method was able to clearly distinguish between individual markers in single sections of tonsil tissue (Figure 1A). Machine-learning assisted analysis allowed for the identification of single cells utilizing the nuclear counterstain image with CD20 membrane boundaries; and the mean intensity of MYC, BCL2, BCL6 and Ki67 could be reliably quantitated at a single-cell resolution. Importantly, the signals could be clearly unmixed to yield single-staining image outputs. From these unmixed images, an

intensity-based threshold was adopted to define each cell as "positive" or "negative" for the given marker of interest. These thresholds were validated by 2 independent expert hematopathologists.

As expected, expression of BCL6 and BCL2 in the CD20+ cells of the benign lymphoid tissue (tonsil) was restricted to the germinal centre (GC) and extra- GC regions respectively. MYC showed sparse positivity in the germinal centre CD20+ cells (Figure 1A). The single-cell resolution approach allowed us to quantify the extent at which all markers co-localised. The co-localisation of MYC, BCL2 and BCL6 in CD20+ cells enables eight theoretical B-cell populations (sub-populations), denoted henceforth as M+2+6+, M+2+6-, M+2-6+, M+2-6-, M-2+6+, M-2+6-, M-2-6+ and M-2-6- (where M is MYC, 2 is BCL2, and 6 is BCL6 and + or - indicates the presence or absence of the marker). Figure 1B demonstrates that the repertoire of sub-populations present in a tonsil is limited, with M-2-6+ being dominant within the germinal centre, and M-2+6- being dominant outside the germinal centre. Hardly any cells displayed co-expression of MYC, BCL2 or BCL6 in the extra-GC and GC compartments.

We then investigated the patterns of these MYC, BCL2 and BCL6-based B-cell sub-populations in DLBCL. We stained for these markers in samples from the National University Hospital cohort (NUH, *n*=152; Supplementary table 1). Whereas in tonsil the localisation of BCL2 and BCL6 in CD20+ cells were clearly restricted to distinct compartments, in DLBCL these proteins frequently localised together (Figure 1C-E). Furthermore, in DLBCL many CD20+ cells had a clear expression of MYC, which often co-localised with both BCL2 and/or BCL6. Importantly, unlike in tonsil tissue, within DLBCL cases the full repertoire of the eight sub-populations was observed (Figure 1D-E). I.e. even within cases that were globally high for MYC, BCL2 and BCL6, these markers were not always found in the same cells.

We then evaluated the percentage extent; i.e the percentage of cells within the tumour visually "positive" or "negative" for a defined marker (or combination of markers), as defined by pathological review and setting of an intensity threshold. The differences between tonsil and DLBCL in terms of percentage extent of sub-populations can be appreciated clearly when comparing Figure 2A with Figure 2B. The normal pattern of mutually exclusive expression between MYC, BCL2 and BCL6 in reactive B-cells is lost in DLBCL, underlining the disruption of regulatory mechanisms controlling expression of these three oncogenes. Staining from both the NUH cohort, and another DLBCL cohort obtained from Chi-Mei Medical Center, Taiwan (CMMC, *n*=150; Supplementary table 1; Supplementary figure 1) revealed that the percentage extent of the sub-populations per tumour was variable among patients, but remarkably similar in

the overall distribution in both cohorts (Figure 2B; Supplementary figure 1). Lymphomas that harbour translocations in MYC, BCL2 and/or BCL6 are termed double hit or triple hit lymphomas (DHL/THL), depending on the number of concurrent translocations (21). This group of lymphomas, like DELs, has a particularly poor outcome (22-25), and are therefore highlighted in Figure 2B. Translocation status, whether single marker or DHL/THL, was not correlated with a high percentage extent of any specific sub-populations (Figure 2B). There was also no correlation of any specific sub-populations to cell-of-origin (COO) status as determined using the IHC-based Hans algorithm (26) (Figure 2B). We also examined the proliferative nature of each sub-population by assessing Ki67-positivity in tonsil tissue and DLBCL samples (Figure 2C). In the tonsil, M-2-6+ B-cells (confined to the germinal centre sublocation) were enriched for Ki67-positivity, consistent with proliferation in the germinal center reaction. Interestingly, in both the NUH and CMMC DLBCL cohorts, the sub-populations positive for BCL6 were again predominantly positive for Ki67. These results highlighting the disconnect between Ki67 and MYC/ BCL2 expression at the single-cell level offer insight into the lack of prognostic significance of Ki67 in DLBCL.

Prognostic significance of MYC/BCL2/BCL6 sub-populations

We next sought to understand whether the sub-populations were differentially associated with prognosis during R-CHOP treatment. For each single-marker and sub-population, we performed a univariate Cox proportional hazards (Cox PH) model analysis using percentage extent as a continuous variable at 5% increments, which allowed an unbiased assessment without having to define an arbitrary cut-off. Among the single markers (independent of co-expression) in the NUH cohort, only BCL2 associated with progression-free survival (PFS); PFS defined as the time from diagnosis to relapse of DLBCL/ last follow-up (Figure 3A). Interestingly, among the different sub-populations, M+2+6- and M-2+6- were statistically significant associated with poorer PFS and overall survival (OS), OS referring to length of time from diagnosis till death/ last follow-up (Figure 3A). We focused on the M+2+6- sub-population as it had a more pronounced hazard ratio as compared to the M-2+6- sub-population, especially in terms of overall survival. We next performed a multivariate analysis to adjust for clinically-relevant clinicopathological parameters, namely IPI Risk Group, COO and MYC FISH status [Supplementary table 2]. The international prognostic index (IPI) is a well-validated prognostic index for DLBCL on R-CHOP treatment: comprising of clinical and biochemical parameters (27,28). Importantly, the hazard ratio for both PFS and OS remained statistically significant for the M+2+6- sub-population (Table 1). As the M+2+6- sub-population remained significantly

associated with survival as a continuous variable, for Kaplan-Meier analyses we dichotomized the population based at an optimal percentage extent cut-off for the population (with a minimum of a quartile). M+2+6- High cases (cases with a tumour that had a high percentage extent the M+2+6- sub-population) showed worse survival when compared to M+2+6- Low cases (cases with a tumour that had a low percentage extent the M+2+6- sub-population) (Figure 3B). Interestingly, this difference was most apparent in the IPI Low-Risk subset of patients (comprising IPI 0 and 1) who typically present an overall favourable prognosis (Figure 3C).

The DEL phenotype in DLBCL is defined in several studies using an overall cut-off of ≥40% MYC positive and ≥50% BCL2 positive cells (9). When using the above definition of DEL in our NUH cohort, we noted a trend towards inferior survival outcome in terms of PFS and OS for DEL cases compared to non-DEL cases (Figure 3D), similar to many published cohorts. As our analysis showed that M+2+6- sub-populations existed even in tumours which did not meet traditional definitions of DEL, we sought to investigate whether this sub-population could be predictive of survival also in non-DEL cases. When stratifying non-DEL cases into M+2+6- percentage extent High and Low, we observe a clear difference in prognosis between the two groups, with the high percentage-extent group having a more adverse outcome (Figure 3E). These findings suggest that the percentage of this sub-population can refine the prediction of poor outcomes even in IPI Low-Risk cases and supersedes the traditional DEL definition based on markers stained separately. As the CMMH cohort did not have clinical outcome data for R-CHOP treated samples, we validated our findings in two additional independent DLBCL cohorts from Singapore General Hospital (SGH, *n*=67; Supplementary table 1; Supplementary figure 1) and MD Anderson Cancer Centre (MDA, *n*=40; Supplementary table 1; Supplementary figure 1). Despite overall variability between the cohorts with respect to individual markers, the M+2+6- sub-population consistently correlated with poor prognosis in both of these validation cohorts (Figure 4A-B, Supplementary table 3). Taken together, these results demonstrate that simultaneous measurement of co-expression of MYC, BCL2 and BCL6 at a single-cell resolution in DLBCL offers a reproducible and prognostically meaningful stratification of tumours.

A probabilistic model based on independent co-localisation accurately predicts MYC, BCL2 and BCL6 co-expression in DLBCL

The expression and localisation pattern of MYC, BCL2 and BCL6 in reactive germinal centres implies the existence of biological processes that restrict expression of each marker to specific topological compartments. These processes were clearly deregulated in DLBCL, with multiple

patterns of MYC, BCL2 and BCL6 co-expression. However, we did observe that the distribution of single marker percentages (extents) are similar in different cohorts of DLBCL cases (Figure 5A, Supplementary figure 2A) and followed a similar consensus distribution within a population of patients (Supplementary figure 2B). We therefore aimed to model the co-expression of these markers in DLBCL. We checked if the observed patterns of co-localisation were a result of each marker being regulated independently of each other or, alternatively, if the expression of one marker influenced the expression of the other i.e. interlinked or inter-related regulation (through either direct or indirect biological mechanisms). Figure 5B provides a schematic depicting the expected percentage extent of each sub-population depending on the above two possibilities. For inter-related expression events, we focused on two extremes - overlapping (markers expressed in the same cell population) or mutually exclusive (markers expressed exclusively in different cell populations). From Figure 1A and B we see that in tonsil tissue sub-populations are mainly restricted to M-2+6-, M-2-6+ and M-2-6- suggesting that localisation of these markers is driven by an inter-related mutually exclusive process (Figure 5B, left). However, in DLBCL, the patterns observed in Figure 1C and D were consistent with an independent expression model (Figure 5B, right).

To quantitatively test this observation, we reasoned that if the co-expression of these oncogenes were independent of each other, the percentage extent of sub-populations could be predicted from the percentage extent of each marker using a simple probabilistic model. Briefly, with such a model, the percentage extent for each individual marker comprising a sub-population can be multiplied together resulting in the percentage extent of the sub-population as a whole (see Methods for further details). If, however the co-expression of the three markers was interlinked, the observed percentage extent of each sub-population in our multiplexed data would deviate from the probabilistic prediction. Interestingly, we observed a highly concordant correlation between observed and predicted percentage extent for each sub-population (Figure 5C, Supplementary figure 3), proving that the co-expression of MYC, BCL2 and BCL6 in given cells within DLBCL is driven by independent events. The implication of these findings are that if the quantitative percentage extent of MYC, BCL2 and BCL6 per case are known, it is possible to calculate the percentage of each sub-population. Interestingly, compared to the non-DHL/THL cases, the predicted percentage extent in DHL/THL cases deviates slightly from the observed percentage (Figure 5D-right). This suggests that in lymphomas with these translocation events, the expression of MYC, BCL2 and BCL6 may by driven in part by an inter-related mechanism as opposed to independently. Given the small number of DHL/THL cases in our cohort and modest effect size, further validation of this phenomenon is required.

Prediction of sub-population extent can be performed on gene expression data

On the basis of the above findings, we hypothesized that it is possible to predict the sub-population percentage extent from any quantitative data measuring MYC, BCL2, BCL6 expression. Indeed, among such quantitative data are gene expression datasets (i.e. microarray or RNA-seq). Given that MYC and BCL2 protein expression correlates at least partially with mRNA expression (29), we sought to validate our finding in modelled RNA datasets. As a discovery set, we utilized RNA expression data from GSE10846 (30) (Supplementary figure 4A). Briefly, the gene expression data for each marker were initially transformed to fit the observed population distribution established from single-cell protein expression analysis depicted in Supplementary figure 2B (Supplementary figure 4B, see Methods). The transformed data (ranging from 0-100) was then used as a surrogate for the percentage positivity for each marker. We then inferred percentage extent of sub-populations based on the mathematical model validated by single-cell protein expression analysis (see Methods and Supplementary table 4). We finally evaluated the association of these sub-populations with survival. As used previously for qIHC cohorts, we performed an unbiased univariate Cox PH for all sub-populations followed by visualization of the dichotomized M+2+6- sub-population in a Kapan-Meier analysis. Remarkably, mRNA-predicted M+2+6- percentage extent associated with poorer OS in the GSE10846 cohort (Figure 6A), similar to the directly measured M+2+6- percentage extent from protein co-expression.

We then applied the same methodology to MYC, BLC2, BLC6 mRNA expression data from additional validation cohorts with R-CHOP survival data, namely GSE32918 (31) and GSE117556 (7). After percentage extent transformation, single marker distribution in all three RNA cohorts followed the empirically established distribution (Supplementary figure 4C, see also Figure 5A and Supplementary figure 2). M+2+6- percentage extent remained the only sub-population consistently associated with poor survival in all cohorts (Figure 6B-C), indicating the robustness of these findings. Using an IHC classification of DEL and non-DEL cases provided by the authors (7) we also performed a subset analysis of M+2+6- in non-DEL cases, similar to our analysis with protein co-expression in the NUH cohort (Figure 3E). Again, even in the non-DEL cases in the Sha et al. cohort, those with high predicted M+2+6- percentage extent had significantly poorer survival (Figure 6C, right panel). The above concordance of results between protein- and mRNA- datasets validates our predictive modelling method. The prognostic significance for other sub-populations and single markers varied across cohorts, consistent with previous meta-analyses of MYC, BCL2 and BCL6 single marker expression (32). However, the

remarkable consistency of the M+2+6- sub-populations associating with poor survival after R-CHOP treatment in DLBCL in three protein-based cohorts and three mRNA-based cohorts highlights its value to inform future biological studies and biomarker development.

Prognostic significance of sub-populations using single marker data from retrospective semi-quantitative IHC staining

Having validated the robustness of our algorithm to estimate prognostic sub-populations from any quantitative single marker data, we wanted to check if this could also be applicable in the setting of clinical-grade semi-quantitative IHC. Chromogenic IHC with manual visual scoring by pathologists remains the most widely used method for assessment of MYC, BCL2 and BCL6 in DLBCL. To do this we utilized a well-studied cohort of DLBCL from British Columbia Cancer (BCC) (22,33) which had percentage scores for MYC, BCL2 and BCL6 graded by three independent pathologists. Unlike the previous cohorts described in this paper (where fluorescent multiplex IHC was used), the BCC cohort was stained using chromogenic IHC for MYC, BCL2 and BCL6 on consecutive sections. We noted that distribution of MYC, BCL2 and BCL6 percentage extent in this cohort (Figure 7A) was different to that of our other fluorescent-IHC cohorts, as expected by the differences in sensitivity of fluorescent vs chromogenic IHC and automated vs manual scoring. Nevertheless, despite obvious differences in marker distribution, we noted a remarkable consistency with previous cohorts in the prognostic significance of sub-populations derived from semi-quantitative single-marker scores. The M+2+6- subpopulation again conferred a poorer prognosis in both a univariate Cox PH analysis as well as a Kaplan-Meier analysis using a dichotomized M+2+6- sub-population (Figure 7B). These data suggest that the algorithm we describe for the prediction of the extent of M+2+6- cells works in multiple different settings where the percentage of each of MYC, BCL2 and BCL6 are available- whether through automated or manual scoring. Importantly- the M+2+6- fraction remains predictive of poor survival in all these settings, highlighting the potential broad applicability of these data.

Discussion

The identification of markers to predict for failure of R-CHOP therapy is paramount to the integration of new agents into the frontline management of DLBCL. Co-expression of the oncogenes MYC and BCL2 have an adverse outcome in DLBCL (9,12-14), and this poor outcome appears to be exacerbated when BCL6 expression is absent (11). So far, these associations have been considered on a whole-tumour scale only, not properly taking into

account associations at the single-cell level. Moreover, these markers are not used for patient stratification due to subjective reporting methods. In this study, we aimed to develop a novel approach to develop a quantitative prognostic marker incorporating information from MYC, BCL2 and BCL6, by evaluating the hitherto unexplored aspect of co-localisation at single-cell resolution. We used multispectral qIHC to circumvent limitations with conventional IHC techniques; staining and visualizing MYC, BCL2 and BCL6 simultaneously in a sample. Of the eight sub-populations constructed from possible permutations of MYC, BCL2 and BCL6 co-localisation; we identified that one in particular, M+2+6-, consistently correlated with poor outcome across three independent cohorts studied at the protein level using multiplex fluorescent IHC and one using sequential chromogenic IHC. The findings from our retrospective study will need to be prospectively validated, but these results offer the possibility of a novel method for analysing MYC, BCL2 and BCL6 expression for prognostic purposes in DLBCL. We propose that the identification of the M+2+6- sub population refines the double expressor classification, by clarifying the phenomenon at single-cell resolution. Importantly, this sub-population can be predicted from even from single marker chromogenic IHC scores, which may extend its applicability in settings where automated platforms may not be available. However, this study was not able to identify a single universal “cut-off” at which this sub-population was most relevant. This is likely due to the variety of methods used in sample preparation across these multiple cohorts, which led to differences in the exact scoring of MYC, BCL2 and BCL6 for each sample set by the automated algorithm. Further prospective work will be required to establish suitable and standardized cutoffs for the M+2+6- percentage extent that is most discriminatory for survival, and this is likely to be different for fluorescent and chromogenic IHC based on our data. Nonetheless, M+2+6- remained consistently the most significant sub-population in continuous proportional hazards models, which robustly attests to the influence of this sub-population on survival. We show here that information on how MYC, BCL2 and BCL6 are co-expressed within single cells in DLBCL is critical to understand how they interact to drive prognosis, and could represent a clinically applicable biomarker for patient stratification in front-line clinical trials of DLBCL.

Why are high numbers of M+2+6- cells bad in DLBCL? At this point we only offer hypotheses. MYC provides competitive advantages in the context of subclonal growth assays (34), and regulates a large number of genes to promote carcinogenesis (35). Its overexpression however makes cells more amenable to apoptosis (36). This apoptotic process can be countered by BCL2 (37) thus providing a mechanistic explanation to why the fraction of cells with co-expression of MYC and BCL2 might result in poorer overall survival after R-CHOP treatment. In

the Eμ-MYC mouse model, BCL2 expression promotes chemoresistance (38), providing another mechanism by which MYC and BCL2 might promote adverse survival. How the absence of BCL6 influences cells with MYC and BCL2 to drive prognosis is interesting. BCL6 is a transcriptional repressor that is expressed at high levels in germinal centre B cells (40,41). Germinal centre B cells are typically associated with high levels of DNA damage due to class-switch recombination and somatic hypermutation (42,43). To enable these processes, BCL6 has the ability to suppress the DNA damage response (DDR) sensors (44,45) p53 (46) and cell cycle inhibitors (39,47,48). It is possible that the absence of BCL6 from MYC/BCL2 positive cells allows the release of BCL6 mediated transcriptional repression of these DDR/ cell cycle genes, enabling them to repair and tolerate chemotherapy induced DNA damage. This study has been performed entirely on treatment-naïve samples. It will be important in the future to determine whether the independent pattern of marker distribution is retained following treatment, or if the tumour reverts to a "steady state" even upon relapse. Further biological work will be required to answer these questions as well as derive therapeutic strategies to counter the poor prognosis conferred.

Finally, we describe a simple algorithm to predict the co-expression of these oncogenes at single cell resolution in DLBCL. We were able to show that, unlike in benign lymphoid tissue, in DLBCL the spatial distribution and co-localisation of these three markers is disordered and independently regulated. The independent nature of this co-localisation allowed us to mathematically predict the percentage extent of sub-populations, with a remarkable concordance to observed single-cell co-expression on multiplex IHC. Using both protein and mRNA expression datasets, we were able to confirm that the M+2+6- subgroup was consistently associated with an unfavourable prognosis. The ability to determine the percentage extent of each sub-population within mRNA datasets is a useful tool that can facilitate a deeper investigation into the mechanisms driving prognosis in multiple cancer types. Large-scale gene expression data is widely performed in clinical samples due to its ease over pan-proteomic analysis. While the concordance between protein and mRNA data is variable, the approach we outline is feasible for situations where there is a) a reasonable correlation between transcript and protein levels and b) availability of a cohort for protein staining, to assess the population distribution of a set of markers and whether they are independently co-expressed. If both these conditions are met, we show that it is feasible to tap into a multitude of gene expression studies available for a given disease, to understand the clinical relevance of specific sub-populations. This approach may be widely applicable to the study of co-expression of prognostic markers in

other cancer types, and help identify gene-gene relationships of biological and clinical significance.

Methods

Patient samples

The discovery cohort of tonsil tissue (*n*=5) and DLBCL (*n*=152) samples along with clinical data were retrieved from the archives of the Department of Pathology, National University Hospital, Singapore (NUH cohort) of patients diagnosed with DLBCL and chronic tonsillitis between 2010 and 2017, as approved by the Singapore NHG Domain Specific Review Board B study protocol (2015/00176). The specimens were fixed in formalin and embedded in paraffin at the time of biopsy/surgical excision. We used benign tonsil tissues as a control for the optimization of markers, because lymphomas evolve from and often retain epitopes present in normal lymphoid cell types. The repertoire of normal lymphoid cell types are well represented in benign tonsil samples (49,50). An additional DLBCL cohort was obtained from the Department of Pathology, Chi-Mei Medical Center, Taiwan (CMMC cohort, *n*=150) to validate the multiplexed qIHC scoring protocol. Two validation DLBCL cohorts with survival data after R-CHOP treatment were obtained from the Department of Haematology, Singapore General Hospital, Singapore (SGH cohort, *n*=67) and from the Department of Hematopathology, MD Anderson Cancer Center, Houston, Texas, USA (*n*=40). Messenger-RNA expression data for MYC, BCL2 and BCL6 was obtained from Gene Expression Omnibus for the following DLBCL datasets GSE10846 (*n*=420) (30), GSE117556 (*n*=928) (7) and GSE32918 (*n*=140) (31). To validate our findings using semi-quantitative IHC with pathologist defined scores we obtained a R-CHOP treated DLBCL cohort from British Columbia Cancer (BCC cohort, n=*316*). For clinicopathological details please see ref. (22) and ref. (22,33). A consort diagram of the study is provided in Supplementary figure 5 and full patient characteristics are provided in Supplementary table 1.

Fluorescence in situ hybridization (FISH) staining

3µm FFPE sections were placed on electrostatically charged slides (Platinum Pro, Matsunami Glass Ind. Ltd, Japan). FISH processing was done using the IntelliFISH Universal FFPE Tissue Pretreatment Kit (Vysis, Downer's Drove, IL, USA) according to the manufacturer's instructions and established laboratory protocol. The sections were then subjected to direct FISH using the Vysis LSI MYC Dual Color (01N63-020), Break-Apart Rearrangement Probe (Vysis, Downer's

Drove, IL, USA). The other 2 probes used are the Vysis LSI BCL2 Dual Color, Break-Apart Rearrangement Probe (05N51-020) and the Vysis LSI BCL6 Dual Color, Break-Apart Rearrangement Probe (1N23-020). Images were obtained using the Olympus BX61 microscope and captured on the Applied Image Analysis System v.3.93 (Applied Imaging, Pittsburgh, PA). A total of 100 non-overlapping, intact interphase nuclei were enumerated. The cut off of >15% was used for a positive result in break-apart FISH.

Quantitative immunohistochemistry (qIHC)

Acquisition of tonsil and DLBCL images was performed with the Vectra 2 multispectral imaging system (PerkinElmer). Multispectral images were analysed inForm 2.4.8 (PerkinElmer); first, single fluorescently stained samples were used to generate a spectral library to define the emission profile of each fluorophore used in the experiment, and an unstained sample was used to generate an emission profile of autofluorescence. These spectral profiles were used to unmix the multiplexed IF samples, and thereby generate single colour images to demonstrate appropriate tissue and cellular localisation of CD20, MYC, BCL2, BCL6 and Ki67. After unmixing of multispectral images, a monochrome counterstaining nuclear component and a CD20 membrane component were used in a machine-learning assisted algorithm to create a cell segmentation mask.

Single-marker scoring

A threshold of positivity, based on the quantified mean fluorescent intensity per cell (as per the cell segmentation mask) of MYC, BCL2, BCL6 and Ki67, was determined by visual inspection by a pathologist on a per-case basis. These thresholds were then applied to determine the percentage extent of positivity for each single-marker per TMA core. In the NUH cohort, a median of two TMA cores was analysed per patient (range 2-7) and a median of 3622 cells was analysed per core (range 199-8128). Assuming independent distribution of positivity between MYC, BCL2 and BCL6, a predicted percentage extent of sub-populations, i.e. permutations of MYC, BCL2, BCL6-positivity and -negativity, can be probabilistically inferred. For sub-populations involving the lack of expression of a marker, the percentage extent of the negative cell population should be applied, e.g. percentage extent of the MYC+BLC2+BCL6- (M+2+6-) sub-population can be calculated as follows:

e.g. $M + 2 + 6 - \% = \left(\frac{MYC\%}{100} \times \frac{BCL2\%}{100} \times \frac{(100 - BCL6\%)}{100}\right) \times 100\%$

Transforming mRNA expression data into % extent

Assuming a defined distribution of percentage extent of MYC, BCL2 and BCL6 single-marker scores in a population of DLBCL cases (Supplementary figure 2B) and agreement between mRNA and protein expression (51) we inferred the percentage extent from quantitative mRNA expression data. The transformation curves were fitted manually using the GSE10846 dataset, and validated in GSE117556 and GSE32918. For gene expression detected with multiple probes, single probes with best matching distribution characteristics were used. Binary logarithm of mRNA reads was used for transformation; MYC expression data was fitted using the following sigmoid function:

$$MYC\% = \frac{1}{1+e^{-0.75\times(MYC-p)}} \times 100\%$$

where *p* denotes 70th percentile value of MYC expression in the dataset. BCL6 expression data was fitted using the following sigmoid function:

$$BCL6\% = \frac{1}{1+e^{-0.6\times(BCL6-p)}} \times 100\%$$

where *p* denotes 27th percentile value of BCL6 expression in the dataset. Since BCL2 percentage extent follows a binomial distribution in the population, BCL2 mRNA expression values were fitted as follows: mRNA expression values were normalized between the 10th and 100th percentile of values (all values below 10th percentile were assumed to be equal zero) reflecting the approximate prevalence of cases with <1 percentage-positivity extent BCL2 IHC stating. The normalized values (BCL2n) were transformed using the following function:

$$BCL2t = \frac{1}{1+70^{-(BCL2n/100)}}$$

and the BCL2t values were normalized within each cohort into 0-100 percentage extent values.

Survival analysis

For Cox proportional hazard (Cox PH) models, all variables satisfied the proportional hazards assumption and clinically relevant clinicopathological variables were included in the multivariate models. Continuous percentage extent variables were used at increments, 0-1% compromising the first 'negative' unit, followed by 5% increments of 1-5%, 5-10% etc. Hazard ratios are displayed per unit (of 5% extent). For Kaplan-Meier analyses, the cohorts were dichotomized to reflect the most optimal stratification. Statistical tests were two-sided and $p \leq 0.050$ was considered as statistically significant without correction. IBM SPSS Statistics 23 software was

used to perform Cox PH analyses, all other analyses were performed using GraphPad Prism 8.4.

Semi-quantitative immunohistochemistry

TMA preparation and staining for MYC, BCL2 and BCL6 for the BCC cohort are described in ref. (22) and ref.(22),(33). Percentage extent of MYC, BCL2 and BCL6 staining was determined independently by two pathologists. Thresholds for overall tumour positivity for a given marker were: 40% for MYC, 50% for BCL2 and 30% for BCL6. When there was a discrepancy in scoring between the two pathologists to the extent that scores were found to be on opposing sides of a positivity threshold, a consensus score was obtained from a third pathologist.

Acknowledgements

The authors acknowledge a Yong Siew Yoon Research Grant to ADJ from the National University Cancer Institute of Singapore towards the purchase of the Vectra 2 multispectral imaging system microscope.

Authorship Contributions

Conceptualization- MMH, SBN, ADJ

Methodology (Experimental and analytical design)- MMH, FS, HC, CT, WJC, SBN, ADJ

Project administration (Coordination of sample provision/ethics approvals) - LX, SDM, LMP

Investigation (Multiplex IHC staining/ imaging) FS, YP, PMH, SNC

Data curation (Collection and curation of clinical data): LX, SDM, LMP, EC, JL, YLC, DWS

Formal analysis (Pathological review of cases): SYT, SSSH, STC, SSC, SBN. PF, AM

Formal analysis (Multiplex analysis) MMH, YP, FS

Formal analysis (Bioinformatics/statistical analysis) MMH, HC, ADJ

Writing – original draft: PJ, MMH, ADJ

Writing – review & editing: PJ, MMH, CT, WJC, SBN, ADJ

References

1. Miao Y, Medeiros LJ, Li Y, Li J, Young KH. Genetic alterations and their clinical implications in DLBCL. Nat Rev Clin Oncol **2019**;16(10):634-52 doi 10.1038/s41571-019-0225-1.
2. Coiffier B, Sarkozy C. Diffuse large B-cell lymphoma: R-CHOP failure—what to do? Hematology **2016**;2016(1):366-78 doi 10.1182/asheducation-2016.1.366.
3. Witzig TE, Tobinai K, Rigacci L, Ikeda T, Vanazzi A, Hino M*, et al.* Adjuvant everolimus in high-risk diffuse large B-cell lymphoma: final results from the PILLAR-2 randomized phase III trial. Ann Oncol **2018**;29(3):707-14 doi https://doi.org/10.1093/annonc/mdx764.
4. Vitolo U, Witzig TE, Gascoyne RD, Scott DW, Zhang Q, Jurczak W*, et al.* ROBUST: First report of phase III randomized study of lenalidomide/R-CHOP (R2-CHOP) vs placebo/R-CHOP in previously untreated ABC-type diffuse large B-cell lymphoma. Hematol Oncol **2019**;37(S2):36-7 doi 10.1002/hon.5_2629.
5. Nowakowski GS, Chiappella A, Witzig TE, Spina M, Gascoyne RD, Zhang L*, et al.* ROBUST: Lenalidomide-R-CHOP versus placebo-R-CHOP in previously untreated ABC-type diffuse large B-cell lymphoma. Future Oncol **2016**;12(13):1553-63 doi 10.2217/fon-2016-0130.
6. Davies A, Cummin TE, Barrans S, Maishman T, Mamot C, Novak U*, et al.* Gene-expression profiling of bortezomib added to standard chemoimmunotherapy for diffuse large B-cell lymphoma (REMoDL-B): an open-label, randomised, phase 3 trial. Lancet Oncol **2019**;20(5):649-62 doi https://doi.org/10.1016/S1470-2045(18)30935-5.
7. Sha C, Barrans S, Cucco F, Bentley MA, Care MA, Cummin T*, et al.* Molecular High-Grade B-Cell Lymphoma: Defining a Poor-Risk Group That Requires Different Approaches to Therapy. J Clin Oncol **2019**;37(3):202-12 doi 10.1200/JCO.18.01314.
8. Younes A, Sehn LH, Johnson P, Zinzani PL, Hong X, Zhu J*, et al.* Randomized Phase III Trial of Ibrutinib and Rituximab Plus Cyclophosphamide, Doxorubicin, Vincristine, and Prednisone in Non-Germinal Center B-Cell Diffuse Large B-Cell Lymphoma. J Clin Oncol **2019**;37(15):1285-95 doi 10.1200/JCO.18.02403.
9. Johnson NA, Slack GW, Savage KJ, Connors JM, Ben-Neriah S, Rogic S*, et al.* Concurrent expression of MYC and BCL2 in diffuse large B-cell lymphoma treated with rituximab plus cyclophosphamide, doxorubicin, vincristine, and prednisone. J Clin Oncol **2012**;30(28):3452-9 doi 10.1200/JCO.2011.41.0985.
10. Hu S, Xu-Monette ZY, Tzankov A, Green T, Wu L, Balasubramanyam A*, et al.* MYC/BCL2 protein coexpression contributes to the inferior survival of activated B-cell subtype of diffuse large B-cell lymphoma and demonstrates high-risk gene expression signatures: a report from The International DLBCL Rituximab-CHOP Consortium Program. Blood **2013**;121(20):4021-31 doi 10.1182/blood-2012-10-460063.
11. Horn H, Ziepert M, Becher C, Barth TFE, Bernd H-W, Feller AC*, et al.* MYC status in concert with BCL2 and BCL6 expression predicts outcome in diffuse large B-cell lymphoma. Blood **2013**;121(12):2253-63 doi 10.1182/blood-2012-06-435842.
12. Riedell PA, Smith SM. Double hit and double expressors in lymphoma: Definition and treatment. Cancer **2018**;124(24):4622-32 doi 10.1002/cncr.31646.
13. Herrera AF, Mei M, Low L, Kim HT, Griffin GK, Song JY*, et al.* Relapsed or Refractory Double-Expressor and Double-Hit Lymphomas Have Inferior Progression-Free Survival After Autologous Stem-Cell Transplantation. J Clin Oncol **2017**;35(1):24-31 doi 10.1200/JCO.2016.68.2740.
14. Green TM, Young KH, Visco C, Xu-Monette ZY, Orazi A, Go RS*, et al.* Immunohistochemical Double-Hit Score Is a Strong Predictor of Outcome in Patients With Diffuse Large B-Cell Lymphoma Treated With Rituximab Plus Cyclophosphamide,

Doxorubicin, Vincristine, and Prednisone. J Clin Oncol **2012**;30(28):3460-7 doi 10.1200/jco.2011.41.4342.
15. Meriranta L, Pasanen A, Alkodsi A, Haukka J, Karjalainen-Lindsberg M-L, Leppä S. Molecular background delineates outcome of double protein expressor diffuse large B-cell lymphoma. Blood Adv **2020**;4(15):3742-53 doi 10.1182/bloodadvances.2020001727.
16. Li S, Lin P, Medeiros LJ. Advances in pathological understanding of high-grade B cell lymphomas. Expert Rev Hematol **2018**;11(8):637-48 doi 10.1080/17474086.2018.1494567.
17. Iqbal J, Greiner TC, Patel K, Dave BJ, Smith L, Ji J*, et al.* Distinctive patterns of BCL6 molecular alterations and their functional consequences in different subgroups of diffuse large B-cell lymphoma. Leukemia **2007**;21(11):2332-43 doi 10.1038/sj.leu.2404856.
18. Gorris MAJ, Halilovic A, Rabold K, van Duffelen A, Wickramasinghe IN, Verweij D*, et al.* Eight-Color Multiplex Immunohistochemistry for Simultaneous Detection of Multiple Immune Checkpoint Molecules within the Tumor Microenvironment. J Immunol **2018**;200(1):347-54 doi 10.4049/jimmunol.1701262.
19. Halse H, Colebatch AJ, Petrone P, Henderson MA, Mills JK, Snow H*, et al.* Multiplex immunohistochemistry accurately defines the immune context of metastatic melanoma. Sci Rep **2018**;8(1):11158 doi 10.1038/s41598-018-28944-3.
20. Huang Y-K, Wang M, Sun Y, Di Costanzo N, Mitchell C, Achuthan A*, et al.* Macrophage spatial heterogeneity in gastric cancer defined by multiplex immunohistochemistry. Nat Commun **2019**;10(1):3928 doi 10.1038/s41467-019-11788-4.
21. Rosenthal A, Younes A. High grade B-cell lymphoma with rearrangements of MYC and BCL2 and/or BCL6: Double hit and triple hit lymphomas and double expressing lymphoma. Blood Rev **2017**;31(2):37-42 doi https://doi.org/10.1016/j.blre.2016.09.004.
22. Ennishi D, Jiang A, Boyle M, Collinge B, Grande BM, Ben-Neriah S*, et al.* Double-Hit Gene Expression Signature Defines a Distinct Subgroup of Germinal Center B-Cell-Like Diffuse Large B-Cell Lymphoma. J Clin Oncol **2019**;37(3):190-201 doi 10.1200/JCO.18.01583.
23. Ott G, Rosenwald A, Campo E. Understanding MYC-driven aggressive B-cell lymphomas: pathogenesis and classification. Blood **2013**;122(24):3884-91 doi 10.1182/blood-2013-05-498329.
24. Sarkozy C, Traverse-Glehen A, Coiffier B. Double-hit and double-protein-expression lymphomas: aggressive and refractory lymphomas. Lancet Oncol **2015**;16(15):e555-e67 doi https://doi.org/10.1016/S1470-2045(15)00005-4.
25. Johnson NA, Savage KJ, Ludkovski O, Ben-Neriah S, Woods R, Steidl C*, et al.* Lymphomas with concurrent BCL2 and MYC translocations: the critical factors associated with survival. Blood **2009**;114(11):2273-9 doi 10.1182/blood-2009-03-212191.
26. Hans CP, Weisenburger DD, Greiner TC, Gascoyne RD, Delabie J, Ott G*, et al.* Confirmation of the molecular classification of diffuse large B-cell lymphoma by immunohistochemistry using a tissue microarray. Blood **2004**;103(1):275-82 doi 10.1182/blood-2003-05-1545.
27. Monti S, Savage KJ, Kutok JL, Feuerhake F, Kurtin P, Mihm M*, et al.* Molecular profiling of diffuse large B-cell lymphoma identifies robust subtypes including one characterized by host inflammatory response. Blood **2005**;105(5):1851-61 doi 10.1182/blood-2004-07-2947.
28. Shipp M, Harrington D, Chairpersons. A Predictive Model for Aggressive Non-Hodgkin's Lymphoma. N Engl J Med **1993**;329(14):987-94 doi 10.1056/nejm199309303291402.
29. Zhang L, Xia B, Guo S, Li X, Qu F, Zhao H*, et al.* Coexpression of MYC and BCL-2 Predicts Inferior Survival in Pgi-DLBCL Treated with CHOP-like Regimen/Rituximab. Blood **2014**;124(21):5404- doi 10.1182/blood.V124.21.5404.5404.

30. Lenz G, Wright G, Dave SS, Xiao W, Powell J, Zhao H*, et al.* Stromal Gene Signatures in Large-B-Cell Lymphomas. N Engl J Med **2008**;359(22):2313-23 doi 10.1056/NEJMoa0802885.
31. Barrans SL, Crouch S, Care MA, Worrillow L, Smith A, Patmore R*, et al.* Whole genome expression profiling based on paraffin embedded tissue can be used to classify diffuse large B-cell lymphoma and predict clinical outcome. Br J Haematol **2012**;159(4):441-53 doi 10.1111/bjh.12045.
32. Li L, Li Y, Que X, Gao X, Gao Q, Yu M*, et al.* Prognostic significances of overexpression MYC and/or BCL2 in R-CHOP-treated diffuse large B-cell lymphoma: A Systematic review and meta-analysis. Sci Rep **2018**;8(1):6267 doi 10.1038/s41598-018-24631-5.
33. Ennishi D, Mottok A, Ben-Neriah S, Shulha HP, Farinha P, Chan FC*, et al.* Genetic profiling of MYC and BCL2 in diffuse large B-cell lymphoma determines cell-of-origin–specific clinical impact. Blood **2017**;129(20):2760-70 doi 10.1182/blood-2016-11-747022.
34. Levayer R, Hauert B, Moreno E. Cell mixing induced by myc is required for competitive tissue invasion and destruction. Nature **2015**;524(7566):476-80 doi 10.1038/nature14684.
35. McMahon SB. Emerging Concepts in the Analysis of Transcriptional Targets of the MYC Oncoprotein:Are the Targets Targetable? Genes & Cancer **2010**;1(6):560-7 doi 10.1177/1947601910379011.
36. Hoffman B, Liebermann DA. Apoptotic signaling by c-MYC. Oncogene **2008**;27(50):6462-72 doi 10.1038/onc.2008.312.
37. Bissonnette RP, Echeverri F, Mahboubi A, Green DR. Apoptotic cell death induced by c-myc is inhibited by bcl-2. Nature **1992**;359(6395):552-4 doi 10.1038/359552a0.
38. Schmitt CA, Lowe SW. Bcl-2 Mediates Chemoresistance in Matched Pairs of Primary Eμ-myc Lymphomas in Vivo. Blood Cells Mol Dis **2001**;27(1):206-16 doi https://doi.org/10.1006/bcmd.2000.0372.
39. Shaffer AL, Yu X, He Y, Boldrick J, Chan EP, Staudt LM. BCL-6 Represses Genes that Function in Lymphocyte Differentiation, Inflammation, and Cell Cycle Control. Immunity **2000**;13(2):199-212 doi https://doi.org/10.1016/S1074-7613(00)00020-0.
40. Cattoretti G, Chang CC, Cechova K, Zhang J, Ye BH, Falini B*, et al.* BCL-6 protein is expressed in germinal-center B cells. Blood **1995**;86(1):45-53 doi 10.1182/blood.V86.1.45.bloodjournal86145.
41. Allman D, Jain A, Dent A, Maile RR, Selvaggi T, Kehry MR*, et al.* BCL-6 expression during B-cell activation. Blood **1996**;87(12):5257-68 doi 10.1182/blood.V87.12.5257.bloodjournal87125257.
42. Muramatsu M, Kinoshita K, Fagarasan S, Yamada S, Shinkai Y, Honjo T. Class Switch Recombination and Hypermutation Require Activation-Induced Cytidine Deaminase (AID), a Potential RNA Editing Enzyme. Cell **2000**;102(5):553-63 doi https://doi.org/10.1016/S0092-8674(00)00078-7.
43. Arakawa H, Hauschild J, Buerstedde J-M. Requirement of the Activation-Induced Deaminase (AID) Gene for Immunoglobulin Gene Conversion. Science **2002**;295(5558):1301-6 doi 10.1126/science.1067308.
44. Ranuncolo SM, Polo JM, Dierov J, Singer M, Kuo T, Greally J*, et al.* Bcl-6 mediates the germinal center B cell phenotype and lymphomagenesis through transcriptional repression of the DNA-damage sensor ATR. Nat Immunol **2007**;8(7):705-14 doi 10.1038/ni1478.
45. Ranuncolo SM, Polo JM, Melnick A. BCL6 represses CHEK1 and suppresses DNA damage pathways in normal and malignant B-cells. Blood Cells Mol Dis **2008**;41(1):95-9 doi https://doi.org/10.1016/j.bcmd.2008.02.003.

46. Phan RT, Dalla-Favera R. The BCL6 proto-oncogene suppresses p53 expression in germinal-centre B cells. Nature **2004**;432(7017):635-9 doi 10.1038/nature03147.
47. Shvarts A, Brummelkamp TR, Scheeren F, Koh E, Daley GQ, Spits H*, et al.* A senescence rescue screen identifies BCL6 as an inhibitor of anti-proliferative p19ARF–p53 signaling. Genes Dev **2002**;16(6):681-6 doi 10.1101/gad.929302.
48. Phan RT, Saito M, Basso K, Niu H, Dalla-Favera R. BCL6 interacts with the transcription factor Miz-1 to suppress the cyclin-dependent kinase inhibitor p21 and cell cycle arrest in germinal center B cells. Nat Immunol **2005**;6(10):1054-60 doi 10.1038/ni1245.
49. Zidan, Jecker, Pabst. Differences in Lymphocyte Subsets in the Wall of High Endothelial Venules and the Lymphatics of Human Palatine Tonsils. Scand J Immunol **2000**;51(4):372-6 doi 10.1046/j.1365-3083.2000.00681.x.
50. Nave H, Gebert A, Pabst R. Morphology and immunology of the human palatine tonsil. Anat Embryol **2001**;204(5):367-73 doi 10.1007/s004290100210.
51. Johnson P, Balasubramanian S, Hodkinson B, Schaffer M, Parisi L, Shreeve SM*, et al.* Clinical Impact of Ibrutinib with R-CHOP in Untreated Non-GCB DLBCL Co-Expressing BCL2 and MYC Genes in the Phase 3 Phoenix Trial. Blood **2019**;134(Supplement_1):354- doi 10.1182/blood-2019-124443.

Tables

Table 1

	Total cases *n*=85, missing values *n*=16			
	PFS		OS	
	HR (95% CI)	*p*-value	HR (95% CI)	*p*-value
Sub-population				
M+2+6- (continuous, per 5% of extent)	1.3 (1.0 to 1.6)	0.021	1.4 (1.1 to 1.8)	0.015
IPI Risk Group		0.608		0.543
Low	Ref.		Ref.	
Low-Intermediate	1.5 (0.45 to 5.0)	0.502	1.2 (0.24 to 6.5)	0.802
High-Intermediate	1.5 (0.54 to 4.1)	0.441	2.0 (0.72 to 6.7)	0.167
High	1.9 (0.73 to 5.1)	0.182	1.9 (0.56 to 6.3)	0.312
Cell of origin		0.818		0.671
GCB	Ref.		Ref.	
non-GCB	1.1 (0.46 to 2.7)		1.3 (0.43 to 3.7)	
MYC FISH status		0.968		0.933
negative	Ref.		Ref.	
positive	0.97 (0.27 to 3.6)		0.94 (0.29 to 4.5)	

Table 1. Multivariate analysis of continuous M+2+6- percentage extent at 5% increments as a predictor of PFS and OS in the NUH cohort of DLBCL (Cox proportional hazards model).

PFS – progression-free survival, OS – overall survival, 95% CI – 95% confidence interval, IPI Risk Group - International Prognostic Index Risk Group, GCB - Germinal center B-cell-like diffuse Large B-cell Lymphoma, FISH - fluorescence in-situ hybridization, NUH – National University Hospital, Singapore, Ref. – reference group.

Figures

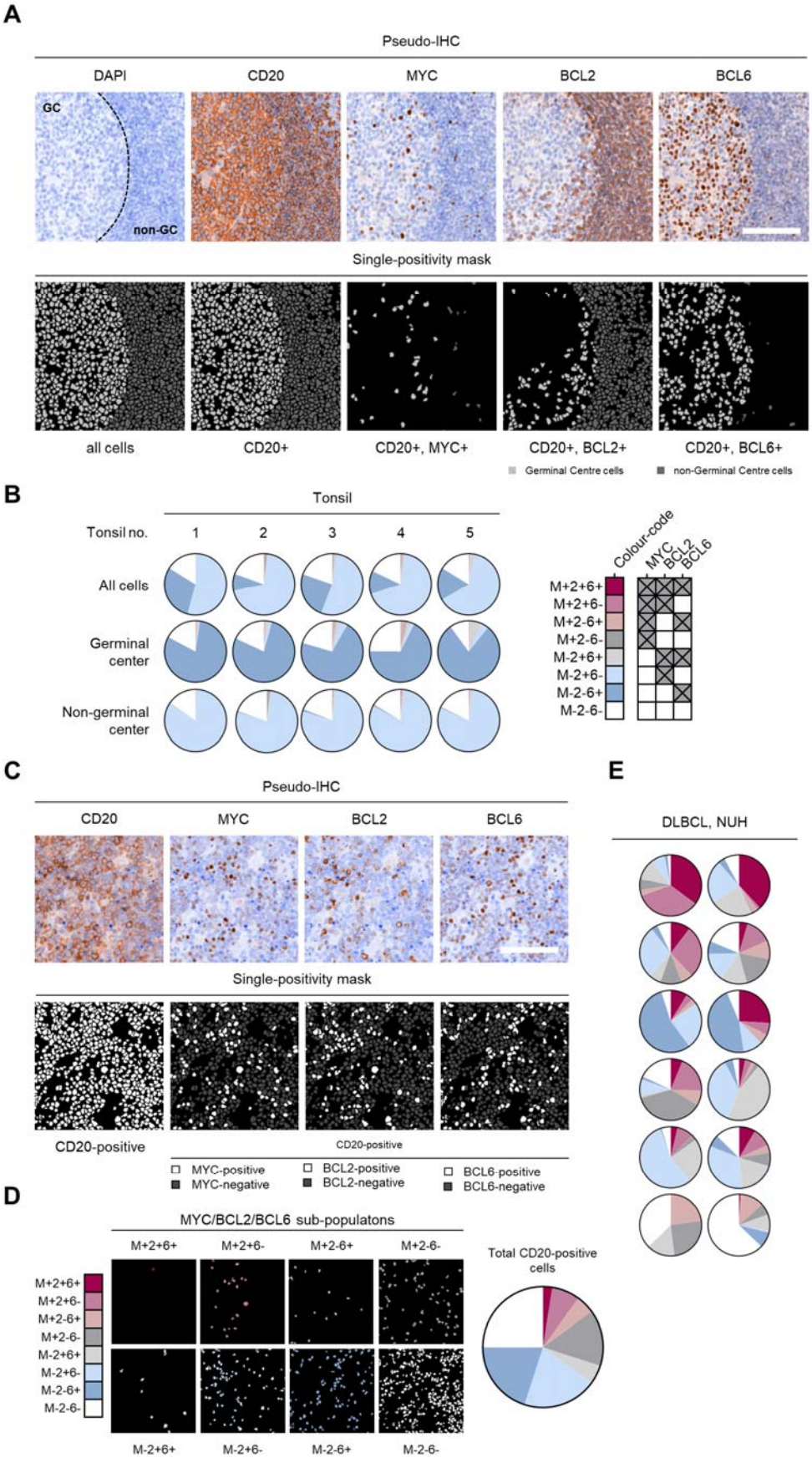

Figure 1

Figure 1. Single-cell MYC, BCL2 and BCL6 protein expression analysis in tonsil and DLBCL tissue. A, Spectrally unmixed false-coloured IF images for CD20, MYC, BCL2 and BCL6 and nuclear counterstaining in tonsil tissue (top panel). The germinal center (GC) and non-germinal center (non-GC) zones are indicated. Cell-segmentation and single-marker positivity masks are shown (bottom panel). Scale bar is 100µm. B, Proportion of sub-populations, i.e. possible permutations of MYC/BCL2/BCL6 positivity and negativity, within tonsil tissues within the CD20-positive cell population. C, Example of DLBCL MYC/BCL2/BCL6 multiplexed IF staining. Spectrally unmixed false-coloured IF images for CD20, MYC, BCL2 and BCL6 are shown (top panel). Cell-segmentation and single-marker positivity masks are shown within the CD20-positive cell population (bottom panel). Scale bar is 100µm. D, Positivity masks of sub-populations in example image from panel (C). E, Proportion of sub-populations measured in twelve example DLBCL cases from the NUH cohort. Colour-coding as in panel (B) and (D).

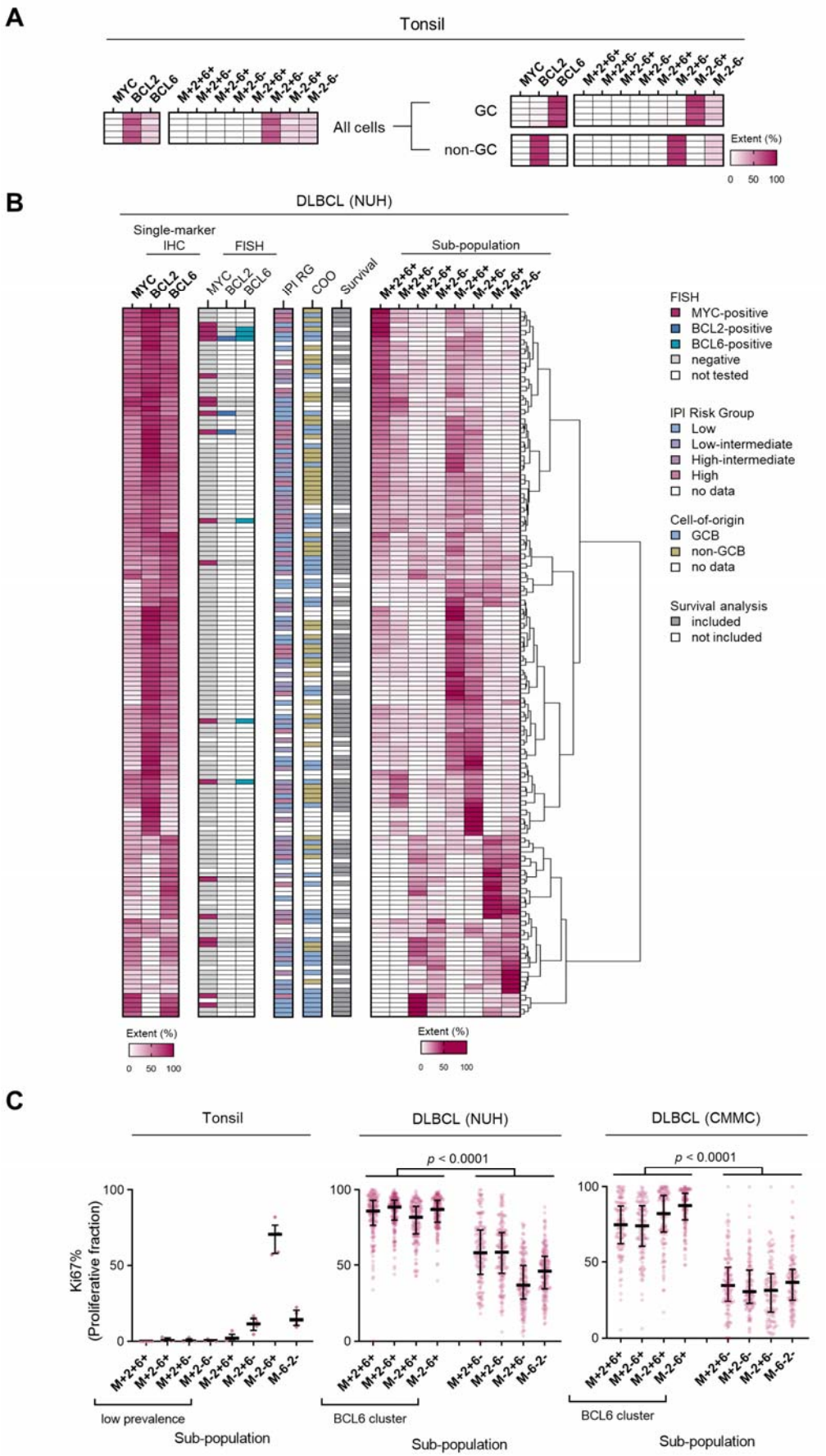

Figure 2

Figure 2. Global distribution of MYC, BCL2 and BCL6 sub-populations with proliferation analysis in DLBCL cohorts. A, Heat-map displaying the percentage extent of individual markers and each sub-population within tonsil tissue. Whole-tissue analysis (left panel) is sub-divided into germinal center (GC) and non-germinal center (non-GC) zones (right panel). Positivity shading for all heat-maps in this panel ranges between 0-100% positivity. B, Overview of percentage extent of individual markers and sub-populations within DLBCL NUH cohort with hierarchical clustering of DLBCL cases according to sub-population extent. Positivity shading for single markers ranges between 0-100% positivity, whereas shading for combination sub-populations ranges between 0-50% positivity. Clinicopathological features for each patient are indicated including: MYC, BCL2 and BCL6 translocation status (FISH); IPI Risk Group (RG); Cell of Origin (COO); and access to survival data (Survival). GCB - germinal center B-cell like lymphoma. C, Proliferation analysis (i.e. Ki67-positivity) among sub-populations in tonsil and DLBCL samples. Note low prevalence of MYC-positive populations in tonsil tissue. BCL6-positive sub-populations are grouped in DLBCL cohorts. Mann Whitney test (BCL6-positive vs. -negative sub-populations), median with interquartile range.

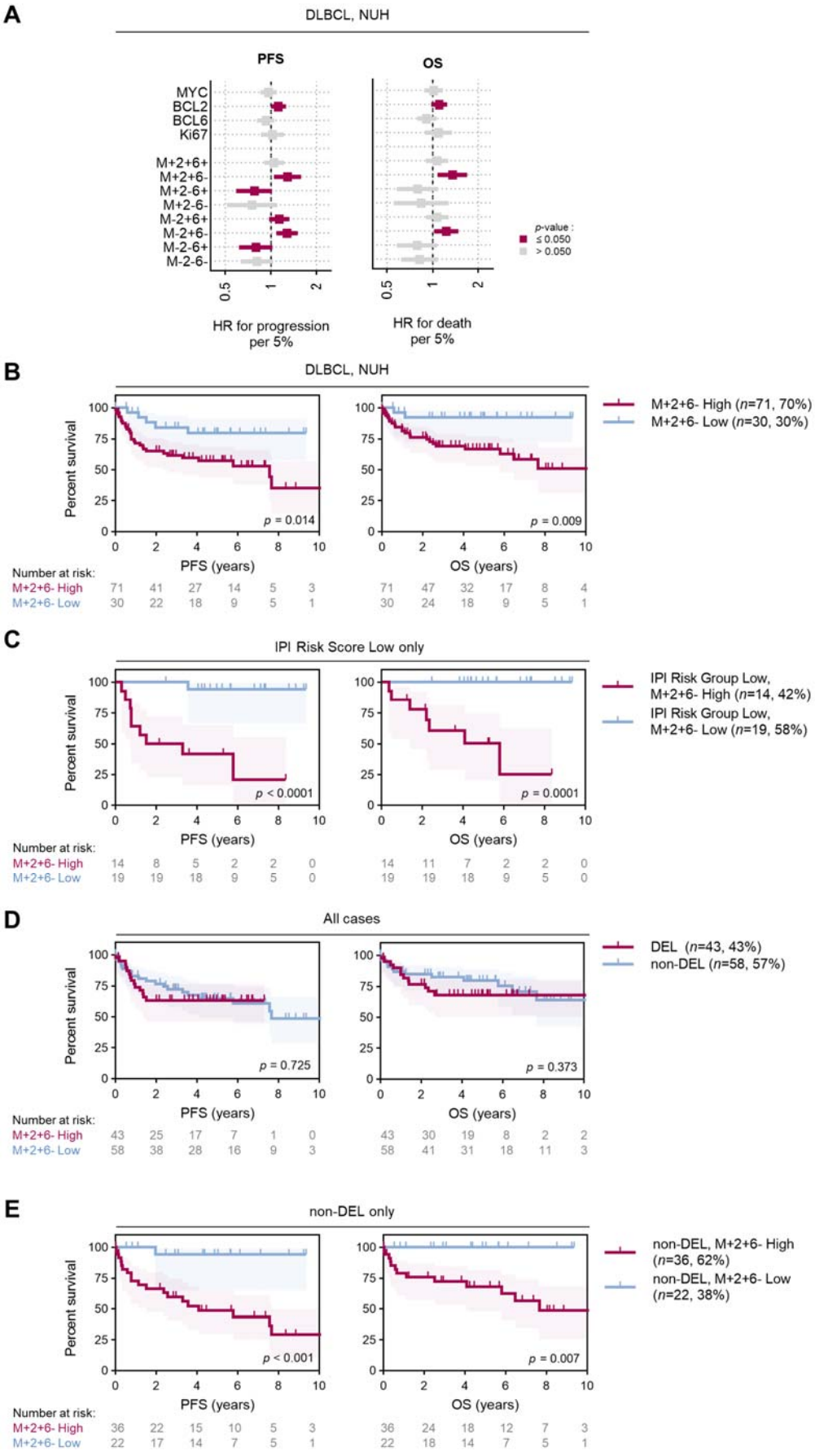

Figure 3

Figure 3. Predictive and prognostic significance of sub-populations. A, Univariate Cox proportional hazards model analysis for MYC, BCL2, BCL6 and Ki67 single-marker and sub-populations percentage extent in the NUH cohort. Percentage-extent was used as a continuous variable in the model at 5% increments (see Methods). PFS – progression-free survival, OS – overall survival. Hazard ratio (HR) with 95% confidence interval per 5%-positivity increment is shown. Kaplan-Meier survival analysis of B, the total NUH cohort and C, IPI Risk Group low subset stratified into M+2+6- High- and Low- groups. D, Kaplan-Meier survival analysis of Double-Expressor Lymphoma (DEL, i.e. MYC ≥ 40% and BCL2 ≥ 50%) cases in the total NUH cohort. E, Non-DEL cases were stratified into M+2+6- High- and Low- groups. Log- rank test, shading denotes 95% confidence interval. Optimal cut-offs were used to stratify B to E into High and Low groups.

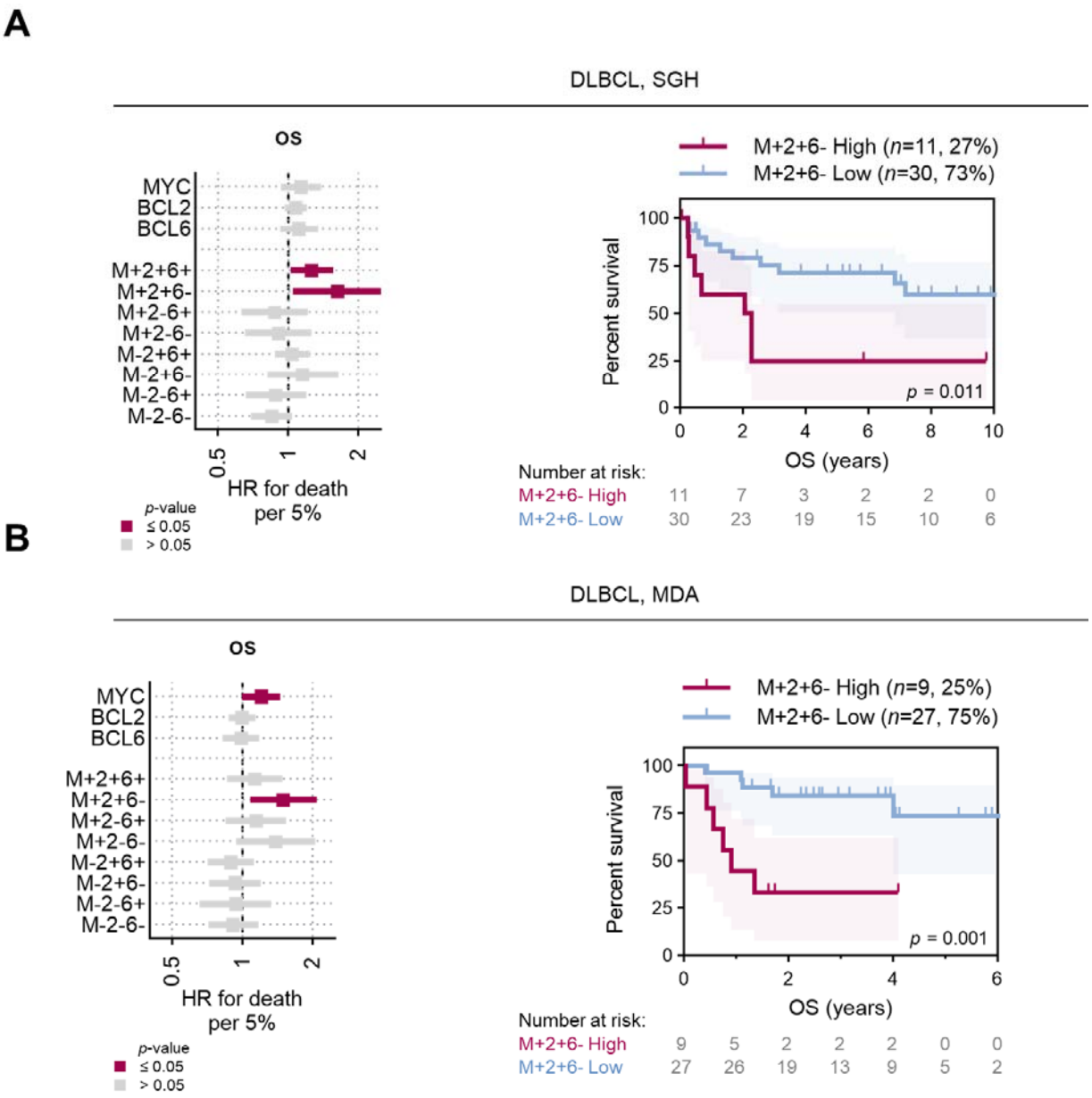

Figure 4. Prognostic significance of sub-populations in validation cohorts. A, Univariate Cox proportional hazards model analysis for MYC, BCL2 and BCL6 single-marker and sub-populations percentage extent in the SGH cohort. Percentage-extent was used as a continuous variable in the model at 5% increments. OS – overall survival; Hazard ratio (HR) with 95% confidence interval per 5%-positivity increment is shown (left panel). Kaplan-Meier survival analysis of the SGH cohort stratified into M+2+6- High- and Low- groups. Log- rank test, shading denotes 95% confidence interval. B, Analysis as in (A) in the MDA cohort. Optimal cut-offs were used to stratify into High and Low groups.

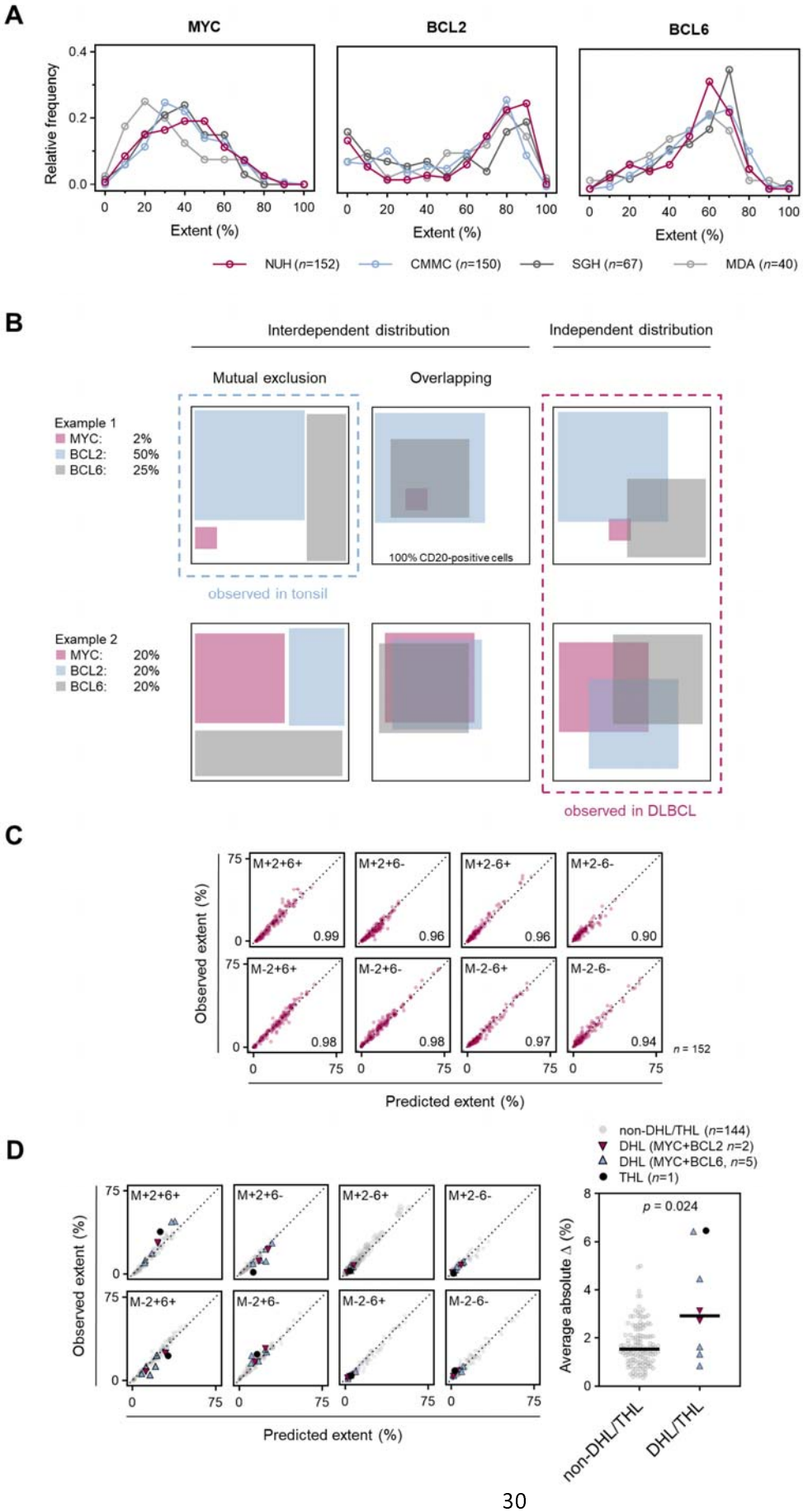

Figure 5

Figure 5. MYC, BCL2 and BCL6 protein expression is independently distributed in cell populations. A, Distribution of single-marker positivity in four DLBCL cohorts as assessed by qIHC (see also Supplementary figure 2). B, Schematics of possible relationships between expression of three markers in a population. The total area within the black box represents 100% of CD20-positive cells within a tumour. Red box represents MYC+ cells, blue box represents BCL2 cells and grey box represents BCL6+ cells. Expression of markers can either present an interdependent distribution, i.e. mutually exclusive or expressed within the same cells; or an indpendent distribution. A mutually exclusive expression relationship is observed between BCL2 and BCL6 in a tonsil. *N.B.: this schematic is not designed to accurately depict the spatial relationships between various co-expressing cell populations* C, Correlation of predicted sub-population percentage extent based on single-marker positivity and observed percentage extent in the NUH cohort. Spearman r. D, Correlation of predicted sub-population percentage extent based on single-marker positivity and observed percentage extent in the NUH cohort as in (C) with lymphomas classified as DHL (MYC+BCL2 or MYC+BCL6) or THL denoted for each sub-population (Left). Scatter plot comparing between non-DHL/THL and DHL/THL cases the absolute difference between predicted percentage extent and observed percentage extent (predicted percentage extent – observed percentage extent) (Right). Mann Whitney test, median.

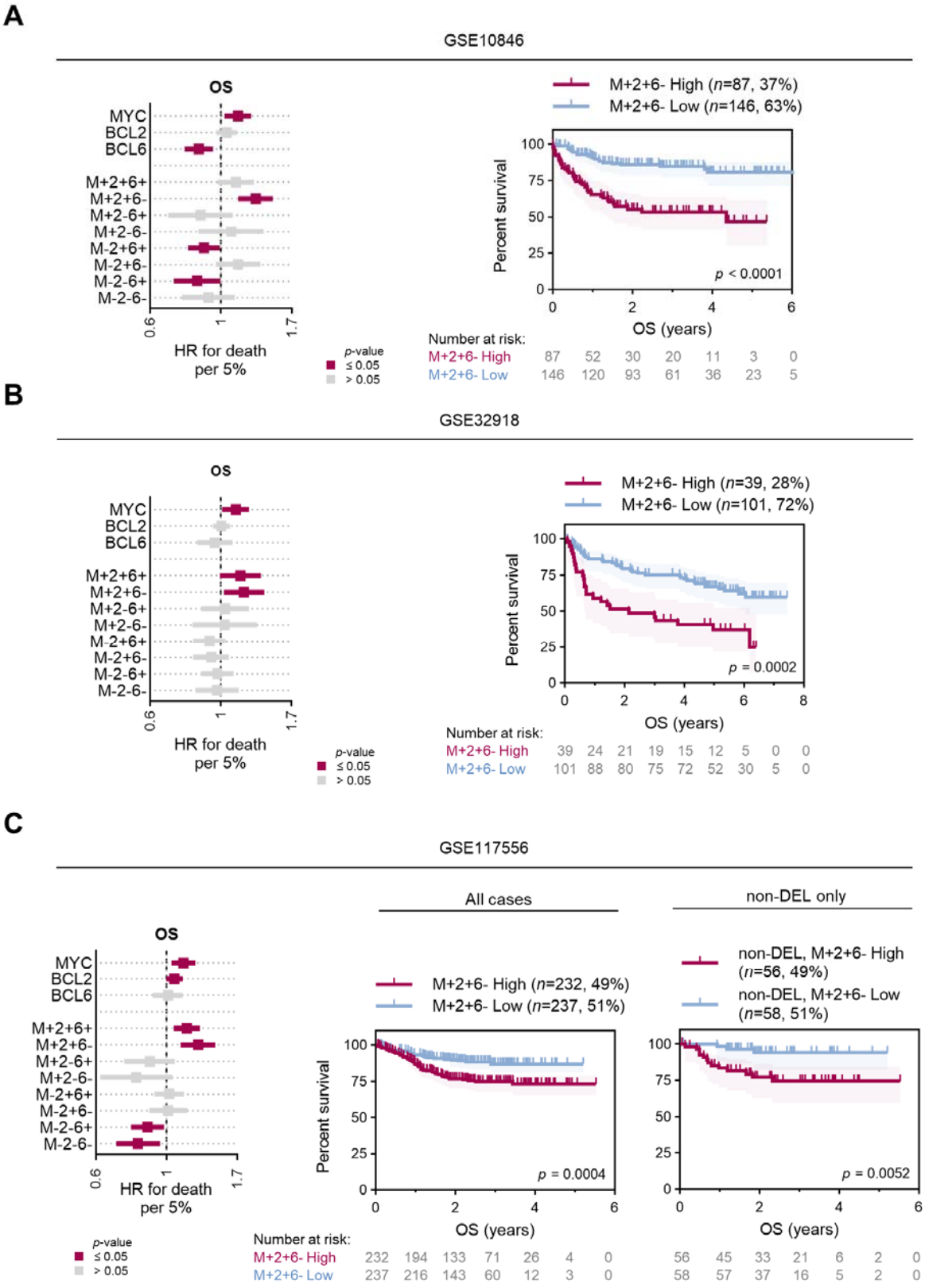

Figure 6

Figure 6. Prognostic impact of inferred MYC, BCL2 and BCL6 sub-populations in mRNA-expression datasets. A, Univariate Cox proportional hazards model analysis for inferred mRNA-based MYC, BCL2 and BCL6 single-marker and sub-populations percentage extent in the GSE10846 cohort. Percentage-extent was used as a continuous variable in the model at 5% increments. OS – overall survival; Hazard ratio (HR) with 95% confidence interval per 5%-positivity increment is shown (left panel). Kaplan-Meier survival analysis of the cohort stratified into M+2+6- High- and Low- groups. Log- rank test, shading denotes 95% confidence interval. B, Having established the mRNA transformation parameters, analysis as in (A) was performed in an additional mRNA cohort - GSE32918. C, Analysis as in (A) in the cohort GSE117556. An additional subset analysis in IHC-defined non-Double Expressor Lymphoma (non-DEL) cases is shown (right panel). Optimal cut-offs were used to stratify into High and Low groups.

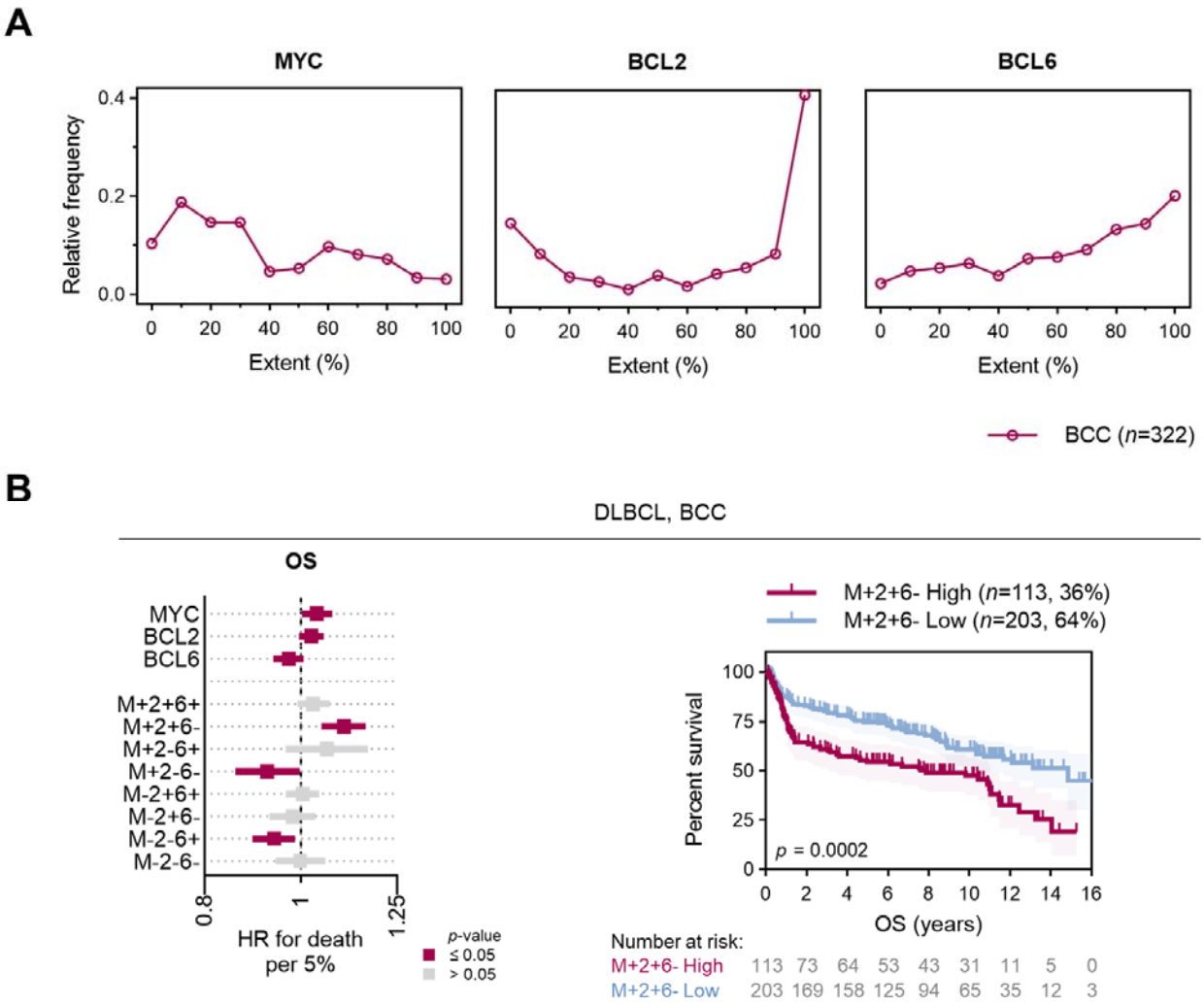

Figure 7. Prognostic significance of sub-populations using single marker data from traditional IHC staining

A, Distribution of single-marker percentage extent for MYC, BCL2 and BCL6 in the BCC cohort as assessed by semi-quantitative IHC. B, Univariate Cox proportional hazards model analysis for MYC, BCL2 and BCL6 single-marker and sub-populations percentage extent in the BCC cohort. Percentage-extent was used as a continuous variable in the model at 5% increments. OS – overall survival; Hazard ratio (HR) with 95% confidence interval per 5%-positivity increment is shown (left panel). Kaplan-Meier survival analysis of the BCC cohort stratified into M+2+6- High- and Low- groups. Log- rank test, shading denotes 95% confidence interval. Optimal cut-offs were used to stratify into High and Low groups.

Supplementary Tables

Supplementary Table 1

Cohort	NUH		CMMC	SGH		MDA	
	Total cases	Survival analysis	Total cases	Total cases	Survival analysis	Total cases	Survival analysis
	n (%)	*n* (%)	*n* (%)	*n* (%)	*n* (%)	*n* (%)	*n* (%)
Total	152 (100%)	101 (100%)	150 (100%)	67 (100%)	41 (100%)	40 (100%)	36 (100%)
IPI Risk Group							
Low	40 (26.3%)	33 (32.7%)	0 (0%)	17 (25.4%)	17 (41.5%)	13 (32.5%)	13 (6.1%)
Low-Intermediate	23 (15.1%)	17 (16.8%)	0 (0%)	10 (14.9%)	10 (24.4%)	6 (15.0%)	6 (16.7%)
High-Intermediate	31 (20.4%)	23 (22.8%)	0 (0%)	6 (9.0%)	6 (14.6%)	7 (17.5%)	7 (19.4%)
High	22 (14.5%)	20 (19.8%)	0 (0%)	5 (7.5%)	5 (12.2%)	10 (25.0%)	10 (27.8%)
No data	36 (23.7%)	8 (7.9%)	150 (100%)	29 (43.3%)	3 (7.3%)	4 (10.0%)	0 (0%)
Cell of origin							
GCB	41 (27.0%)	44 (43.6%)	36 (24.0%)	0 (0%)	0 (0%)	20 (50.0%)	20 (55.5%)
non-GCB	38 (25.0%)	44(43.6%)	91 (60.7%)	0 (0%)	0 (0%)	15 (40.0%)	15 (41.7%)
No data	73 (48.0%)	13 (12.8%)	23 (15.3%)	67 (100%)	41 (100%)	5 (10.0%)	1 (2.8%)
MYC FISH status							
Negative	124 (81.6%)	84 (83.2%)	0 (0%)	0 (0%)	0 (0%)	26 (65.0%)	26 (72.2%)
Positive	19 (12.5%)	13 (12.9%)	0 (0%)	0 (0%)	0 (0%)	8 (20.0%)	8 (22.2%)
No data	9 (5.9%)	4 (3.9%)	150 (100%)	67 (100%)	41 (100%)	6 (15.0%)	2 (5.6%)
BCL2 FISH status							
Negative	16 (10.5%)	11 (10.9%)					
Positive	3 (2%)	2 (2.0%)					
No data	133 (87.5%)	88 (87.1%)					
BCL6 FISH status							
Negative	13 (8.6%)	8 (7.9%)					
Positive	6 (3.9%)	5 (5.0%)					
No data	133 (87.5%)	88 (87.1%)					
Biopsy							
Primary	104 (68.4%)	101 (100%)	0 (0%)	67 (100%)	41 (100%)	40 (100%)	36 (100%)
Relapsed	28 (18.4%)	0 (0%)	0 (0%)	0 (0%)	0 (0%)	0 (0%)	0 (0%)
No data	20 (13.2%)	0 (0%)	150 (100%)	0 (0%)	0 (0%)	0 (0%)	0 (0%)

Supplementary Table 1. Clinicopathologic characteristics of DLBCL patient cohorts evaluated by quantitative immunofluorescence (qIHC).

IPI Risk Group – International Prognostic Index Risk Group, GCB - Germinal center B-cell-like diffuse Large B-cell Lymphoma, FISH - fluorescence in-situ hybridization, NUH – National University Hospital, CMMC - Chi-Mei Medical Center, SGH – Singapore General Hospital, MDA – MD Anderson Cancer Center.

Supplementary table 2

	Total cases *n*=93, missing values *n*=8			
	PFS		OS	
	HR (95% CI)	*p*-value	HR (95% CI)	*p*-value
IPI Risk Group		0.351		0.315
Low	Ref.		Ref.	
Low-Intermediate	1.4 (0.48 to 4.2)	0.523	0.73 (0.15 to 3.6)	0.701
High-Intermediate	1.5 (0.56 to 3.9)	0.425	2.0 (0.70 to 5.7)	0.200
High	2.3 (0.93 to 5.5)	0.071	2.1 (0.75 to 6.1)	0.157
	Total cases *n*=88, missing values *n*=13			
	PFS		OS	
	HR (95% CI)	*p*-value	HR (95% CI)	*p*-value
Cell of origin		0.150		0.071
GCB	Ref.		Ref.	
non-GCB	1.7 (0.82 to 3.6)		2.3 (0.93 to 5.7)	
	Total cases *n*=97, missing values *n*=4			
	PFS		OS	
	HR (95% CI)	*p*-value	HR (95% CI)	*p*-value
MYC FISH status		0.632		0.571
negative	Ref.		Ref.	
positive	0.75 (0.23 to 2.5)		0.62 (0.15 to 2.6)	

Supplementary table 2

	Total cases *n*=93, missing values *n*=8			
	PFS		OS	
	HR (95% CI)	*p*-value	HR (95% CI)	*p*-value
IPI Risk Group		0.351		0.315
Low	Ref.		Ref.	
Low-Intermediate	1.4 (0.48 to 4.2)	0.523	0.73 (0.15 to 3.6)	0.701
High-Intermediate	1.5 (0.56 to 3.9)	0.425	2.0 (0.70 to 5.7)	0.200
High	2.3 (0.93 to 5.5)	0.071	2.1 (0.75 to 6.1)	0.157
	Total cases *n*=88, missing values *n*=13			
	PFS		OS	
	HR (95% CI)	*p*-value	HR (95% CI)	*p*-value
Cell of origin		0.150		0.071
GCB	Ref.		Ref.	
non-GCB	1.7 (0.82 to 3.6)		2.3 (0.93 to 5.7)	
	Total cases *n*=97, missing values *n*=4			
	PFS		OS	
	HR (95% CI)	*p*-value	HR (95% CI)	*p*-value
MYC FISH status		0.632		0.571
negative	Ref.		Ref.	
positive	0.75 (0.23 to 2.5)		0.62 (0.15 to 2.6)	

Supplementary table 2. Univariate analysis of clinicopathological features as a predictors of PFS and OS in the NUH cohort of DLBCL (Cox proportional hazards model).

PFS – progression-free survival, OS – overall survival, 95% CI – 95% confidence interval, IPI Risk Score - International Prognostic Index Risk Score, GCB - Germinal center B-cell-like diffuse Large B-cell Lymphoma, FISH - fluorescence in-situ hybridization, NUH – National University Hospital, Singapore, Ref. – reference group.

Supplementary table 3

Cohort	SGH			MDA	
	Total cases, *n*=37			Total cases, *n*=36	
	OS			OS	
	HR (95% CI)	*p*-value		HR (95% CI)	*p*-value
Sub-population					
M+2+6- (continuous, per 5% of extent)	1.6 (1.1 to 2.5)	0.030	M+2+6- (continuous, per 5% of extent)	1.5 (1.1 to 2.3)	0.025
IPI Risk Group		0.007			0.608
Low	Ref.			Ref.	
Low-Intermediate	2.5 (0.44 to 14.9)	0.299		no events	
High-Intermediate	10.7 (1.8 to 62.2)	0.008		2.5 (0.34 to 14.9)	0.401
High	11.7 (2.1 to 64.8)	0.005		3.5 (0.55 to 23.0)	0.185
Cell of origin		-			0.785
GCB	-	-		Ref.	
non-GCB	-	-		0.79 (0.15 to 4.2)	
MYC FISH status		-			0.480
negative	-	-		Ref.	
positive	-	-		1.8 (0.34 to 9.7)	

Supplementary table 3. Multivariate analysis of continuous M+2+6- % extent at 5% increments as a predictor of PFS and OS in the SGH and MDA cohorts of DLBCL (Cox proportional hazards model).

OS – overall survival, 95% CI – 95% confidence interval, IPI Risk Group – International Prognostic Index Risk Group, SGH – Singapore General Hospital, MDA – MD Anderson Cancer Center, Ref. – reference group.

Supplementary Table 4 – in separate PDF file

Supplementary Table 4. Quantitative prediction of MYC, BCL2, BCL6 and their sub-population percentage extent in mRNA expression DLBCL datasets.

Supplementary table 5

Procedure	Reagent (dilution/product number)	Duration (min.)
1st primary antibody incubation	anti-Bcl-6 (1:30)	60
1st secondary antibody incubation	anti-Mouse HRP (DAKO K4001)	10
1st signal amplification and fluorophore deposition	TSA Opal 670 (1:100)	10
2nd epitope retrieval (antibody stripping)	pH 9 HIER (low power)	10
2nd epitope blocking	BSA	10
2nd primary antibody incubation	anti-Bcl-2 (1:50)	60
2nd secondary antibody incubation	anti-Mouse HRP	10
2nd signal amplification and fluorophore deposition	TSA Opal 520 (1:100)	10
3rd epitope retrieval (antibody stripping)	pH 9 HIER (low power)	10
3rd epitope blocking	BSA	10
3rd primary antibody incubation	anti-c-Myc (1:50)	30
3rd secondary antibody incubation	anti-Rabbit HRP (DAKO K4003)	10
3rd signal amplification and fluorophore deposition	TSA Opal 570 (1:100)	10
4th epitope retrieval (antibody stripping)	pH 9 HIER (low power)	10
4th epitope blocking	BSA	10
4th primary antibody incubation	anti-CD 20 (1:2000)	30
4th secondary antibody incubation	anti-Mouse HRP	10
4th signal amplification and fluorophore deposition	TSA Opal 540 (1:100)	10
5th epitope retrieval (antibody stripping)	pH 9 HIER (high power)	5
5th epitope retrieval (continued)	pH 9 HIER (low power)	10
5th epitope blocking	BSA	10
5th primary antibody incubation	anti-Ki67 (1:50)	45
5th secondary antibody incubation	anti-Mouse HRP	10
5th signal amplification and fluorophore deposition	TSA Opal 620 (1:100)	10
Final antibody stripping	pH 9 HIER (low power)	10
Counterstaining	DAPI (1:50)	5
Mounting	CC mount (Sigma C9368)	10

Supplementary Table 5. Multiplexed immunofluorescence staining procedures.

HRP – horseradish peroxidase, TSA – tyramide signal amplification, HIER – heat-induced epitope retrieval, BSA – bovine serum albumin, DAPI – 4′,6-diamidino-2-phenylindole.

Supplementary table 6

Antibody	Clone	Source	Product Number
anti-CD20	L26	DAKO	M0755
anti-c-Myc	Y69	Abcam	ab32072
anti-Bcl-2	124	DAKO	M0887
anti-Bcl-6	LN22	Leica	NCL-564
anti-Ki67	MIB-1	DAKO	M7240
anti-CD10	56C6	Leica	NCL-270
anti-MUM1	MUM1p	DAKO	M7259

Supplementary Table 6. Antibodies used in this study.

Supplementary Figures

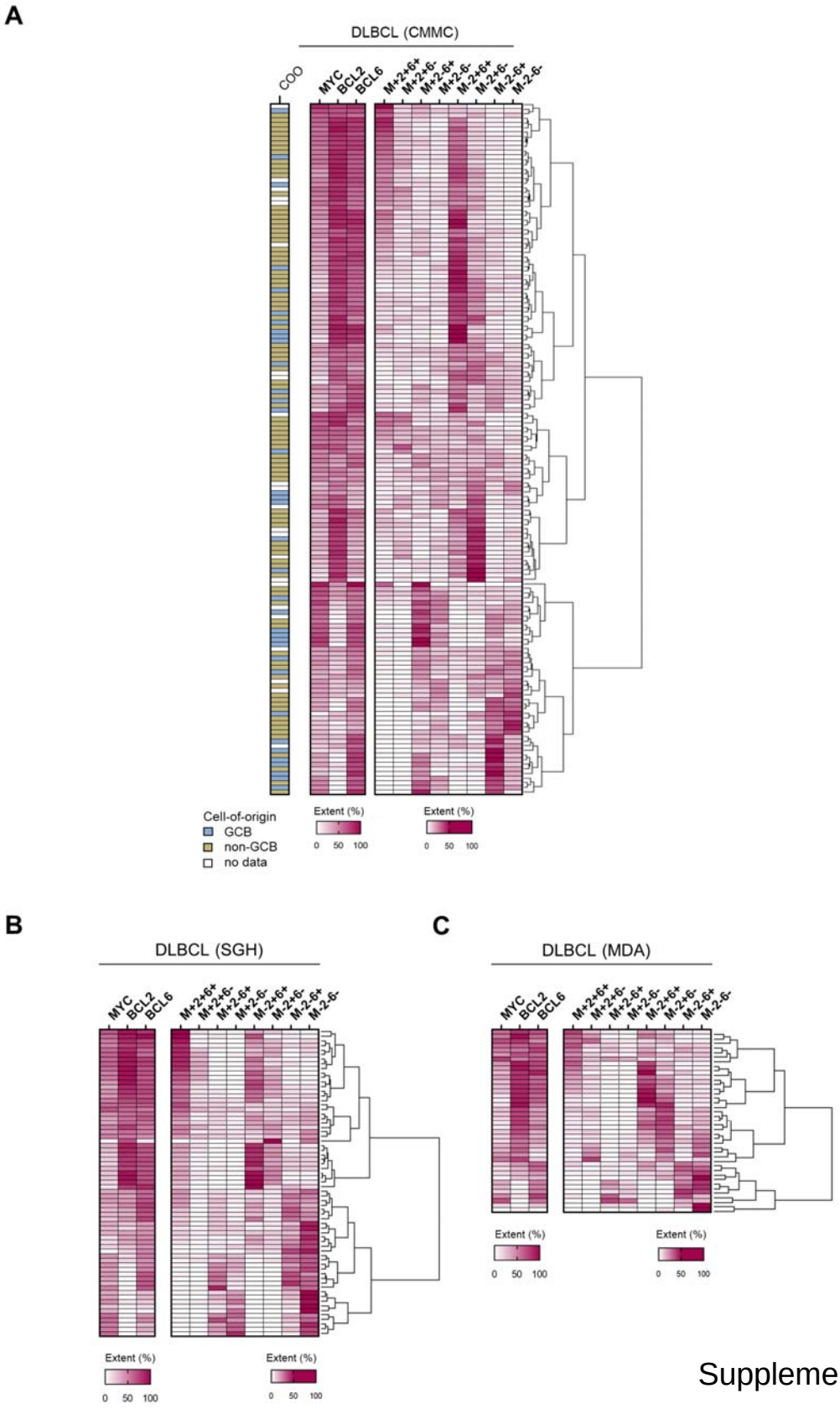

Supplementary figure 1

Supplementary figure 1. Global distribution of MYC, BCL2 and BCL6 sub-populations within validation DLBCL cohorts. A, Heat-map displaying the percentage extent of individual markers and each sub-population within the DLBCL CMMC cohort with hierarchical clustering of DLBCL cases according to sub-population extent. COO status is included. Positivity shading for single markers ranges between 0-100% positivity, whereas shading for combination sub-population ranges between 0-50% positivity. B, Analysis as in (A) in the DLBCL SGH cohort, excluding COO status. C, Analysis as in (A) in the DLBCL MDA cohort, excluding COO status.

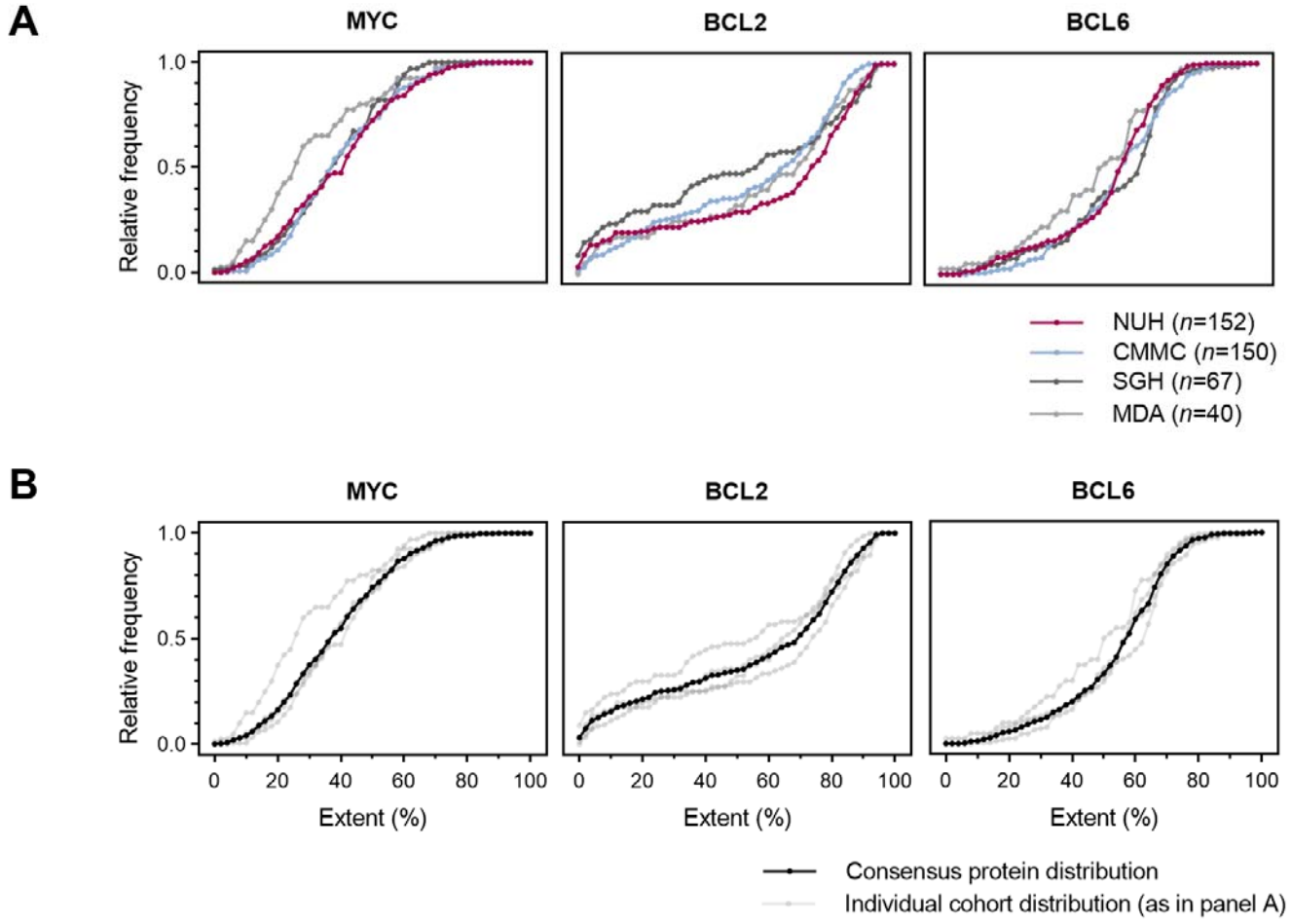

Supplementary figure 2. Percentage extent positivity of MYC, BCL2 and BCL6 single-markers in DLBCL. A, Cumulative histogram of MYC, BCL2 and BCL6 protein percentage extent positivity in DLBCL cohorts (data transformed from Figure 5A). B, A consensus single-marker cumulative distribution of MYC, BCL2 and BCL6 protein percentage extent positivity across all measured protein cohorts.

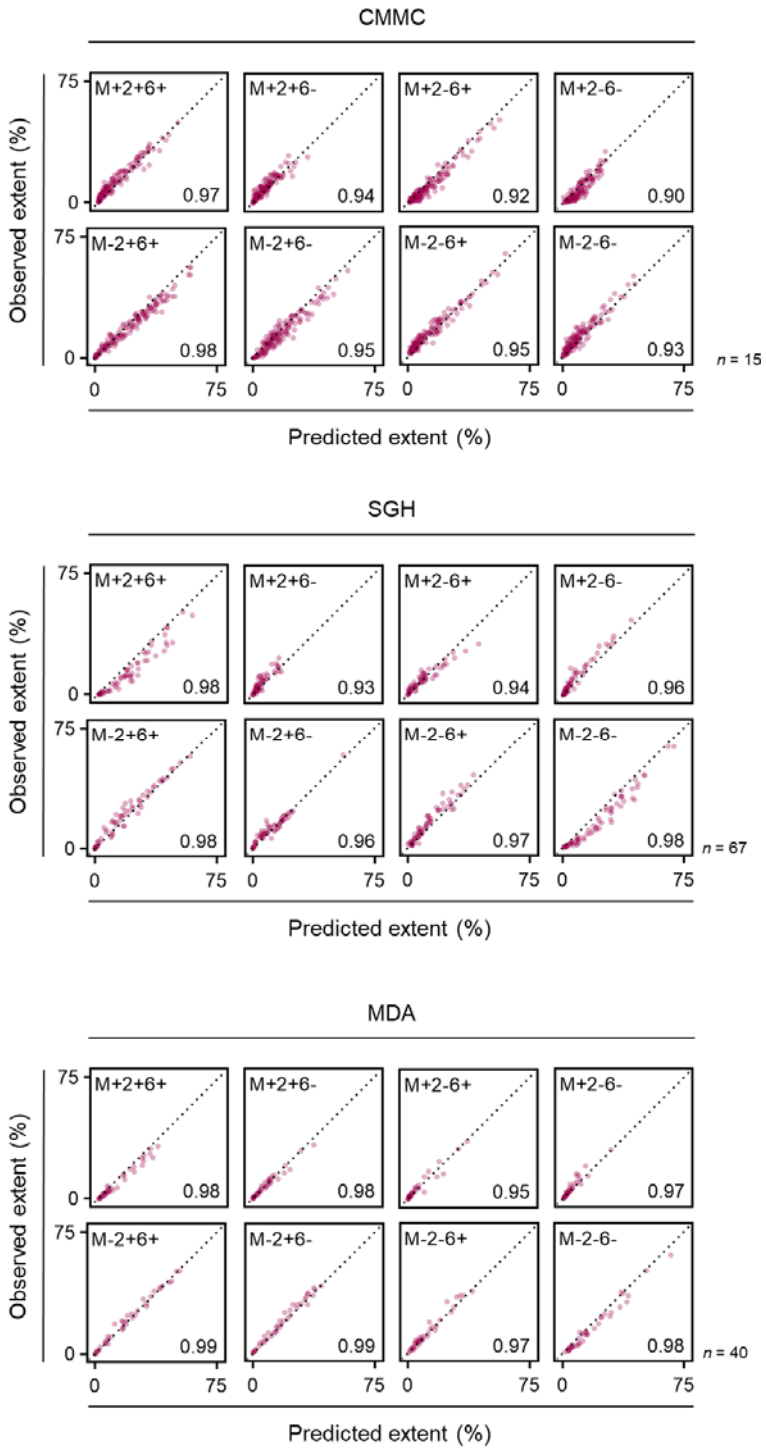

Supplementary figure 3. Correlation of predicted MYC, BCL2 and BCL6 sub-population percentage extent based on single-marker positivity and observed percentage extent in the DLBCL cohorts. Spearman r.

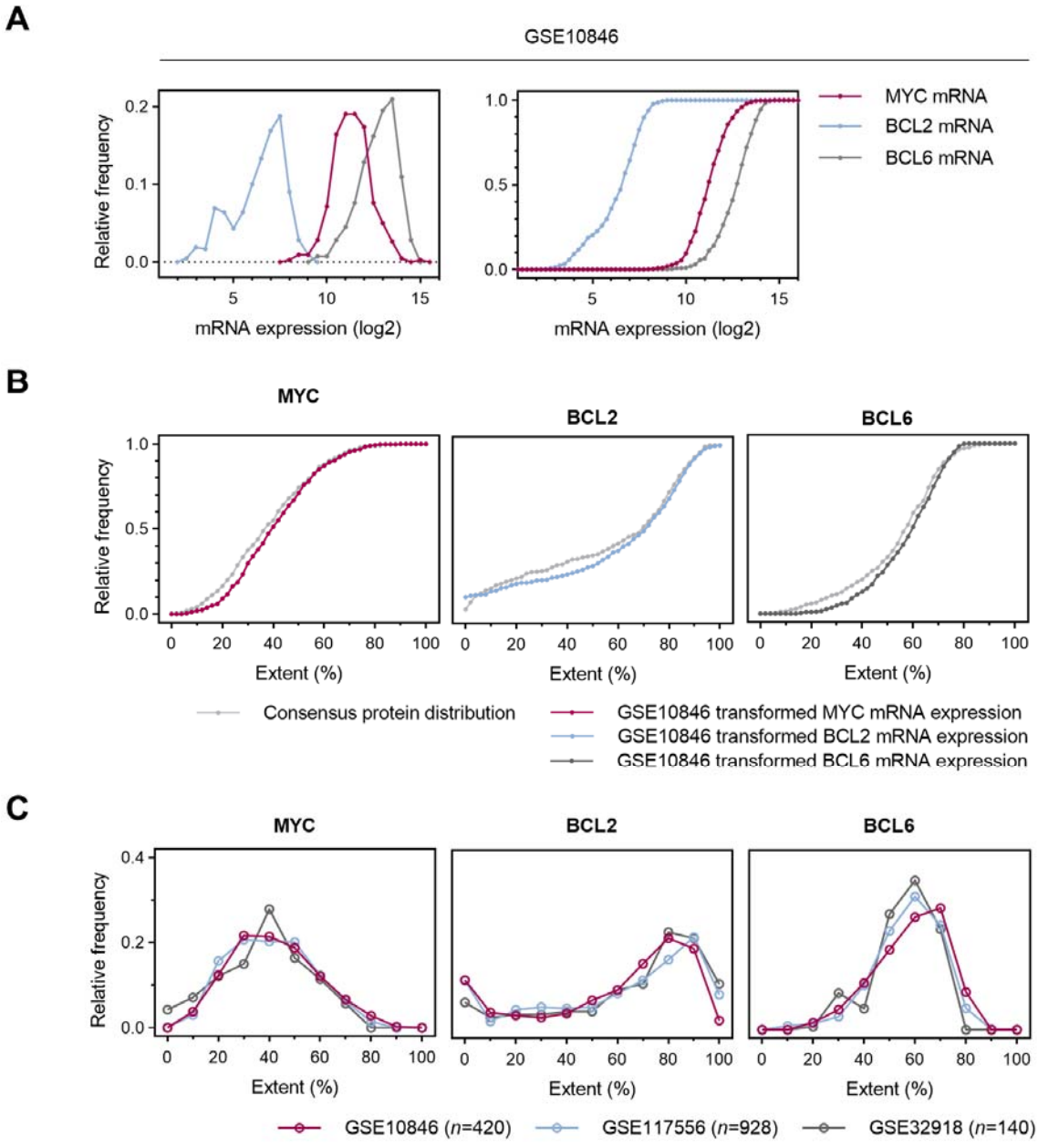

Supplementary figure 4. Inference of percentage extent positivity of MYC, BCL2 and BCL6 single-markers from mRNA-expression data. A, Histogram (left panel) and cumulative histogram (right panel) of mRNA expression of single-markers in the GSE10846 cohort. B, Distribution of transformed mRNA expression of markers in (A) to approximate the measured consensus protein distribution. C, Distribution of transformed single-marker percentage extent from three mRNA expression datasets.

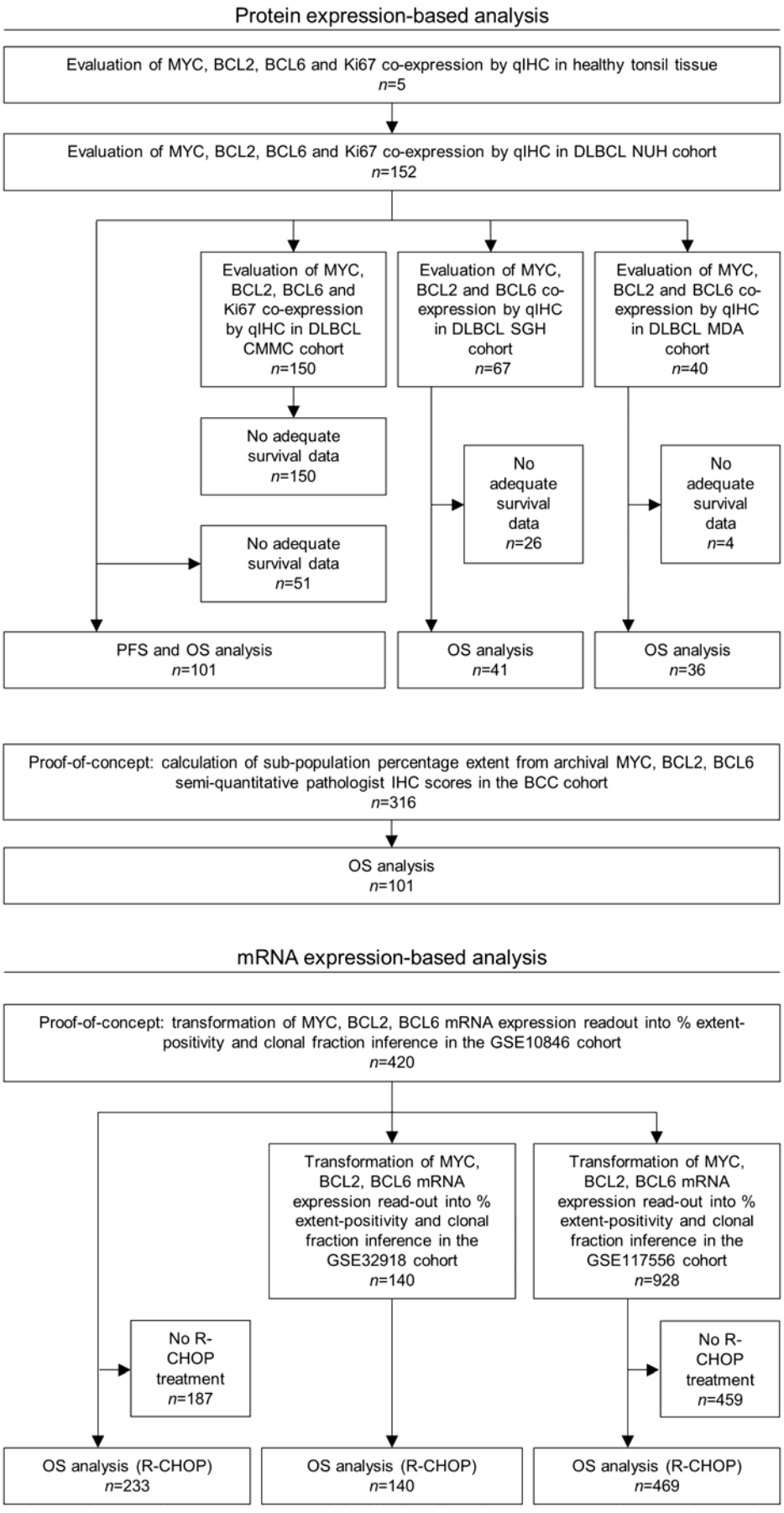

Supplementary figure 5

Supplementary figure 5. Flow-chart of analyses performed in this study. NUH – National University Hospital, CMMC - Chi-Mei Medical Center, SGH – Singapore General Hospital, MDA – MD Anderson Cancer Center, BCC – British Columbia Cancer, qIHC – quantitative immunohistochemistry, PFS – progression-free survival, OS – overall survival, R-CHOP – rituximab, cyclophosphamide, doxorubicin hydrochloride, vincristine, prednisolone.